Phe-Met-Arg-Phe-amide Activates a Novel Voltage-dependent K^+ Current through a Lipoxygenase Pathway in Molluscan Neurones

K.S. Kits, J.C. Lodder, and M.J. Veerman

From the Graduate School Neurosciences Amsterdam, Research Institute of Neuroscience, Vrije Universiteit, Faculty of Biology, 1081 HV Amsterdam, Netherlands

ABSTRACT The neuropeptide Phe-Met-Arg-Phe-amide (FMRFa) dose dependently (ED_{50} = 23 nM) activated a K^+ current in the peptidergic caudodorsal neurones that regulate egg laying in the mollusc *Lymnaea stagnalis*. Under standard conditions ($[K^+]_o$ = 1.7 mM), only outward current responses occurred. In high K^+ salines ($[K^+]_o$ = 20 or 57 mM), current reversal occurred close to the theoretical reversal potential for K^+. In both salines, no responses were measured below −120 mV. Between −120 mV and the K^+ reversal potential, currents were inward with maximal amplitudes at ∼−60 mV. Thus, U-shaped current–voltage relations were obtained, implying that the response is voltage dependent. The conductance depended both on membrane potential and extracellular K^+ concentration. The voltage sensitivity was characterized by an e-fold change in conductance per ∼14 mV at all $[K^+]_o$. Since this result was also obtained in nearly symmetrical K^+ conditions, it is concluded that channel gating is voltage dependent. In addition, outward rectification occurs in asymmetric K^+ concentrations. Onset kinetics of the response were slow (rise time ∼650 ms at −40 mV). However, when FMRFa was applied while holding the cell at −120 mV, to prevent activation of the current but allow activation of the signal transduction pathway, a subsequent step to −40 mV revealed a much more rapid current onset. Thus, onset kinetics are largely determined by steps preceding channel activation. With FMRFa applied at −120 mV, the time constant of activation during the subsequent test pulse decreased from ∼36 ms at −60 mV to ∼13 ms at −30 mV, confirming that channel opening is voltage dependent. The current inactivated voltage dependently. The rate and degree of inactivation progressively increased from −120 to −50 mV. The current is blocked by internal tetraethylammonium and by bath-applied 4-aminopyridine, tetraethylammonium, Ba^{2+}, and, partially, Cd^{2+} and Cs^+. The response to FMRFa was affected by intracellular GTPγS. The response was inhibited by blockers of phospholipase A_2 and lipoxygenases, but not by a cyclo-oxygenase blocker. Bath-applied arachidonic acid induced a slow outward current and occluded the response to FMRFa. These results suggest that the FMRFa receptor couples via a G-protein to the lipoxygenase pathway of arachidonic acid metabolism. The biophysical and pharmacological properties of this transmitter operated, but voltage-dependent K^+ current distinguish it from other receptor-driven K^+ currents such as the S-current- and G-protein-dependent inward rectifiers.

KEY WORDS: Phe-Met-Arg-Phe-amide • S-K current • potassium channel • G-protein • arachidonic acid

INTRODUCTION

K^+ channels are a major target of inhibitory synaptic transmitters and neuropeptides. Gating of postsynaptic receptor-driven K^+ channels may directly depend on G-proteins or involve second messenger pathways (see reviews by Brown, 1990; Brown and Birnbaumer, 1990; Clapham, 1994; Wickman and Clapham, 1995). Examples of the first category are offered by various G-protein-activated inward rectifier K^+ channels (GIRKs),[1] such as the cardiac muscarinic K^+ channels (reviewed by Kurachi et al., 1992; Kurachi, 1995) and dopamine-activated K^+ channels in rat substantia nigra neurons (Kim et al., 1995) and lactotrophs (Einhorn et al., 1991; Einhorn and Oxford, 1993), and possibly striatal neurons (Greiff et al., 1995*a*, 1995*b*). Gating of GIRKs is believed to involve a direct action of the βγ subunit on the channel (Logothetis et al., 1987; Wickman et al., 1994; Kunkel and Peralta, 1995). Related to GIRKs, and to some extent also directly regulated by G-protein α subunits (Terzic et al., 1994), are the ATP/ADP-dependent $I_{K\text{-}ATP}$ channels in heart cells, neurones, and pancreatic β cells (see reviews by Nichols and Lederer, 1991; Takano and Noma, 1993; Terzic et al., 1995). Examples of postsynaptic receptor-driven K^+ channels that are gated through second messengers are the S-K channels in *Aplysia* (reviewed by Belardetti and Siegelbaum, 1988), which are regulated through arachidonic acid and cAMP. In the case of GIRKs, the inward rectifying properties of the channels result in enhanced effectiveness of transmission at near resting membrane

Address correspondence to Dr. K.S. Kits, Graduate School Neurosciences Amsterdam, Research Institute of Neuroscience, Vrije Universiteit, Faculty of Biology, De Boelelaan 1087, 1081 HV Amsterdam, Netherlands. Fax: 20 4447123; E-mail: ksk@bio.vu.nl

[1]*Abbreviations used in this paper:* 4-AP, 4-aminopyridine; 4-bpb, 4-bromophenacylbromide; AA, arachidonic acid; CDC, caudodorsal neurone; FMRFa, Phe-Met-Arg-Phe-amide; GIRK, G-protein-activated inward rectifier K^+ channel; HBS, HEPES buffered saline; I-V, current–voltage; NDGA, nordihydroguaiaretic acid; TEA, tetraethylammonium.

potentials. On the other hand, the second messenger-dependent, but largely voltage-independent, S-K channels also contribute to the repolarizing phase of the action potential.

Members of the Phe-Met-Arg-Phe-NH_2 (FMRFa) family of neuropeptides are putative neurotransmitters in vertebrates and invertebrates (Brussaard et al., 1988; Raffa, 1988). In the molluscan central nervous system, FMRFa acts on K^+ channels in sensory, motor-, and neuroendocrine neurones. Notably, in sensory neurons of *Aplysia*, FMRFa stimulates the S-K current (Belardetti and Siegelbaum, 1988) through activation of the arachidonic acid pathway (Buttner et al., 1989), while, in addition, it activates protein phosphatase-1 (Endo et al., 1995), thus counteracting a phosphorylating pathway, activated by serotonin and acting through PKA that suppresses S-K channels (Sweatt et al., 1989). The largely voltage independent S-K channel (Shuster et al., 1991) is further reported to be stretch sensitive (Vandorpe et al., 1994). S-K or S-K-like current responses were also reported in other identified neurons in *Aplysia* (Brezina et al., 1987) and in *Helisoma* (Bahls et al., 1992). In various other cases, however, it is unclear whether similar K^+-dependent responses to FMRFa and other transmitters involve S-K channels (Sasaki and Sato, 1987; Belkin and Abrams, 1993; Brezina et al., 1994). It seems clear, however, that alternative pathways (i.e., not involving arachidonic acid) are employed to activate similar K^+ currents in different neurones (Bolshakov et al., 1993; Kehoe, 1995).

We have analyzed in detail the properties of the FMRFa-activated K^+ current ($I_{K\text{-}F}$) in the caudodorsal neurones (CDCs) of the mollusc *Lymnaea stagnalis*, using the whole cell voltage clamp approach. CDCs, which control egg laying by secreting an egg-laying hormone (Vreugdenhil et al., 1988), form a homogenous set of neuroendocrine cells in the central nervous system and were previously demonstrated to be strongly inhibited by FMRFa (Brussaard et al., 1988) acting through a specific receptor (Brussaard et al., 1989). We report here that FMRFa activates a novel K^+ current that is characterized by a combined voltage- and receptor-dependent gating mechanism, with both factors being necessary for opening of the channels. In addition, we probed the signal transduction pathway between receptor and channel and report that the response appears to involve the formation of arachidonic acid and its metabolites.

MATERIALS AND METHODS

Animals and Preparation

Adult *L. stagnalis* (20–30-mm shell height), bred in our laboratory, were used. They were kept under a 12–12 h light–dark regimen at 20°C. For all experiments, isolated cells in primary culture were used. To isolate the cells, the central nervous system was dissected and incubated for 40 min at 35°C in medium containing 2 mg/ml trypsin (type 3; Sigma Chemical Co., St. Louis, MO). To check that the FMRFa receptors were not strongly affected by this treatment, some isolations were performed after incubation at room temperature in medium containing 1.33 mg/ml collagenase/dispase (Boehringer Mannheim, Mannheim, Germany) and 0.67 mg/ml trypsin. Next, dissociation was performed by careful mechanical dissection with forceps and a fine needle. Dissociated cells were held in 3 ml HEPES buffered saline (HBS; see below) in tissue culture dishes (Costar Corp., Cambridge, MA) for at least 1 h. Before start of the experiments, the bath volume was reduced to 1.5 ml and experiments were done with constant perfusion (~2 ml/min).

Salines and Drugs

Unless otherwise stated, the experiments were done in HBS containing (mM): 30 NaCl, 1.7 KCl, 10 $NaCH_3SO_4$, 5 $NaHCO_3$, 4 $CaCl_2$, 1.5 $MgCl_2$, 10 HEPES, pH 7.8, adjusted with 7 mM NaOH. In addition, two high potassium salines were used. 20 K^+-HBS contained 20 mM KCl, replacing 20 mM NaCl. In 57 K^+-HBS, 50 mM KCl replaced all NaCl, $NaCH_3SO_4$, and $NaHCO_3$, while pH was adjusted with 7 mM KOH. For whole-cell voltage clamp recordings, a pipette medium was used, containing (mM): 29 KCl, 2.3 $CaCl_2$, 2 MgATP, 0.1 TrisGTP, 11 EGTA, 10 HEPES, pH 7.4, adjusted with 35–38 mM KOH.

FMRFa was obtained from Peninsula Laboratories Europe Ltd. (St. Helens, UK), guanosine 5′-*O*(3-thiotrisphosphate) lithium salt (GTPγS) from Boehringer Mannheim, and 4-aminopyridine (4-AP), 4-bromophenacylbromide (4-bpb), nordihydroguaiaretic acid (NDGA), and indomethacin from Sigma Chemical Co. FMRFa was applied to the cell by means of Y-tube application. The Y-tube system allows rapid, gravity-driven application of a saline through a pipette, which is positioned close to the cell. Driven by negative pressure, a continuous flow of saline is transported through the pipette to a waste chamber. Switching of an electrically operated valve disrupts this flow and opens the arm that is connected to open air, releasing the negative pressure and allowing the saline to flow out of the pipette, over the cell. To measure the rapidity of this system, we applied a high potassium saline (57 mM K^+) via the Y-tube system to a cell bathed in low potassium saline (1.7 mM K^+). This local change in driving force for potassium results in a rapid change in holding current, being a direct measure for the change of the potassium concentration. Y-tube application proved rather rapid, reaching 90% of its final level in 171 ± 33 ms ($n = 5$). Wash of the saline took place in 4.8 ± 0.5 s ($n = 3$).

4-AP, 4-bpb, NDGA, and indomethacin were applied to the cell by bath perfusion and, where appropriate, also added to the FMRFa solution. Stocks of these blockers (except for 4-AP, which was diluted in distilled water) were made in DMSO in a concentration of 10^{-1} M. Final concentration of DMSO in the bath was 0.01% for 4-bpb and 0.005% for NDGA and indomethacine. GTPγS was applied by adding it to the pipette medium, replacing TrisGTP.

Electrophysiological Recordings

Whole cell voltage clamp recordings were made using an 8900 amplifier (Dagan Corp., Minneapolis, MN) with a 1- or 10-GΩ feedback resistance, or an Axoclamp 200A amplifier (Axon Instruments, Foster City, CA).

Electrodes were pulled on a Flaming/Brown P-87 puller (Sutter Instruments, Co., Novato, CA) and heat polished, resulting in electrodes with resistances of 4–6 MΩ, yielding seal resistances of 4–10 GΩ. The series resistance (6–10 MΩ) was compensated for

~70%. With current amplitudes being <1 nA, the maximal resulting voltage error did not exceed 3 mV. To reduce fast capacitances, the pipettes were coated with Sylgard (Dow Corning, Seneffe, Belgium). Voltage protocols, data acquisition, and analysis were computer controlled using a 1401 AD/DA interface (CED, Cambridge, UK), employing software developed in our laboratory or using a Digidata 1200 with pCLAMP 6 software (Axon Instruments). Samples of 1,024 points or more per sweep were taken and stored on floppy disk. In most experiments, the currents were filtered at 100 Hz. For the tail current measurements (see Fig. 4) and the experiments on activation kinetics (see Fig. 5), high sampling rates and filtering frequencies were used.

Unless otherwise stated, data are presented as means ± SEM.

RESULTS

FMRFa activates a K^+ current. Under current clamp conditions, FMRFa caused a hyperpolarization accompanied by a decrease in input resistance of the cells, while the reversal potential depended on $[K^+]_o$, indicating that the response is due to opening of K^+ channels (Brussaard et al., 1988). Under voltage clamp, application of FMRFa elicited an outward current with slow kinetics when applied at voltages positive to −80 mV. The response to FMRFa was dose dependent (Fig. 1). The threshold for activation of the current was 10^{-9} M, the ED_{50} was 2.3×10^{-8} M, and the response saturated at 10^{-6} M ($n = 5$). Unless otherwise stated, we applied FMRFa at 10^{-6} M in all subsequent experiments.

To construct a current–voltage (I-V) relation, we applied a voltage protocol with a holding potential of −60 mV from which pulses ranging from −120 to 0 mV in 10-mV steps were given. After the onset of the voltage step, we waited 10 s before application of FMRFa was started to allow voltage-dependent currents, gated at voltages above −30 mV, to settle to a steady state. The response amplitude was then measured as the maximal current during FMRFa application minus the current directly preceding application of the peptide.

The resulting current voltage relation (Fig. 2, *A* and *B*) shows that only outward current responses were recorded and that the current did not reverse (voltage range −120 to 0 mV). To confirm the presumed K^+ selectivity of the response, we determined if the current reversed in high extracellular K^+ concentrations. With 20 mM K^+ in the outside medium, the current reversed at −24.4 ± 1.1 mV ($n = 6$), close to the theoretical reversal potential for K^+ of −29 mV (Fig. 2, *C* and *D*). Bathed in a K^+ concentration of 57 mM K^+, the current reversed at −5.2 ± 1.1 mV ($n = 7$), again close to the theoretical K^+ reversal potential of −3 mV (Fig. 2, *E* and *F*). Furthermore, when all intracellular K^+ ions were substituted by Cs^+ ions, no outward current was seen upon application of FMRFa. Finally, several K^+ channel blockers blocked the FMRFa response (see below). We conclude from these results that FMRFa activated a K^+ current.

Voltage dependence of activation. In standard HBS (1.7 mM K^+), the FMRFa-activated current did not reverse. This might be due to (*a*) outward rectification due to the K^+ gradient, and (*b*) voltage dependence of the current. To distinguish between these hypotheses, we compared the I-V relations in standard HBS, 20 K^+-HBS, and 57 K^+-HBS (Fig. 2). In both high K^+ salines, reversal of $I_{K\text{-}F}$ was observed, but a strong asymmetry between inward and outward currents remained. However, this asymmetry clearly differs from the asymmetry predicted by the Goldman-Hodgkin-Katz equation (see Hille, 1994) on the basis of the K^+ gradient (Fig. 2, *B*, *D*, and *F*). Notably, we observed U-shaped I-V relations at 20 and 57 mM $[K^+]_o$, while the Goldman-Hodgkin-Katz equation predicts monotonously increasing relations between I and V. The decreasing current amplitude at

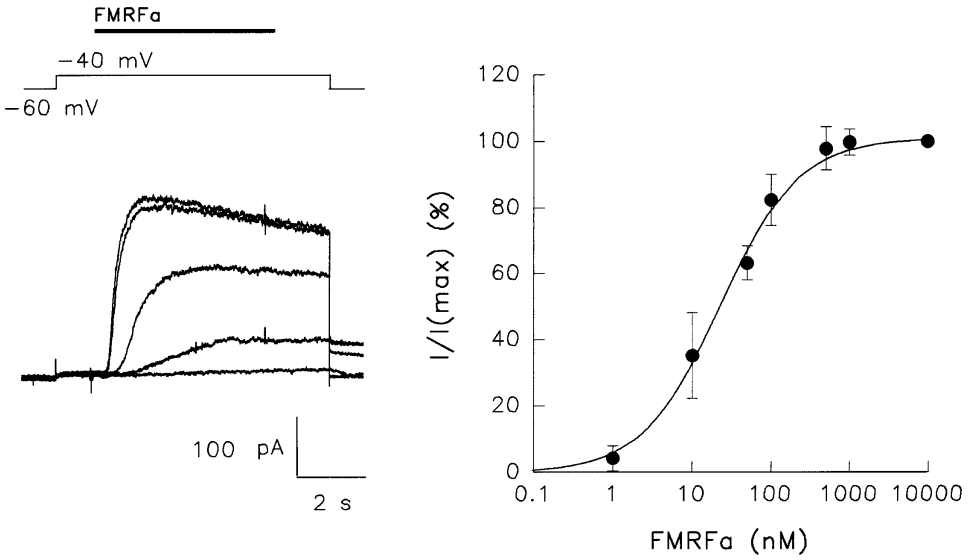

FIGURE 1. Dose dependence of the FMRFa response. (*left*) FMRFa was applied at concentrations of 10^{-9}, 10^{-8}, 5×10^{-8}, 10^{-7}, and 5×10^{-7} M during a voltage step to −40 mV to yield outward current responses of increasing amplitude. Pulse protocol: thin lines indicate voltage step from −60 to −40 mV, bar indicates timing of the FMRFa pulse. Artifacts in the current traces are caused by switching of the Y-tube valve. (*right*) Dose–response curve of FMRFa. The fitted line has an ED_{50} of 2.3×10^{-8} M and a Hill coefficient of 0.9; (vertical bars indicate ±SEM; $n = 5$).

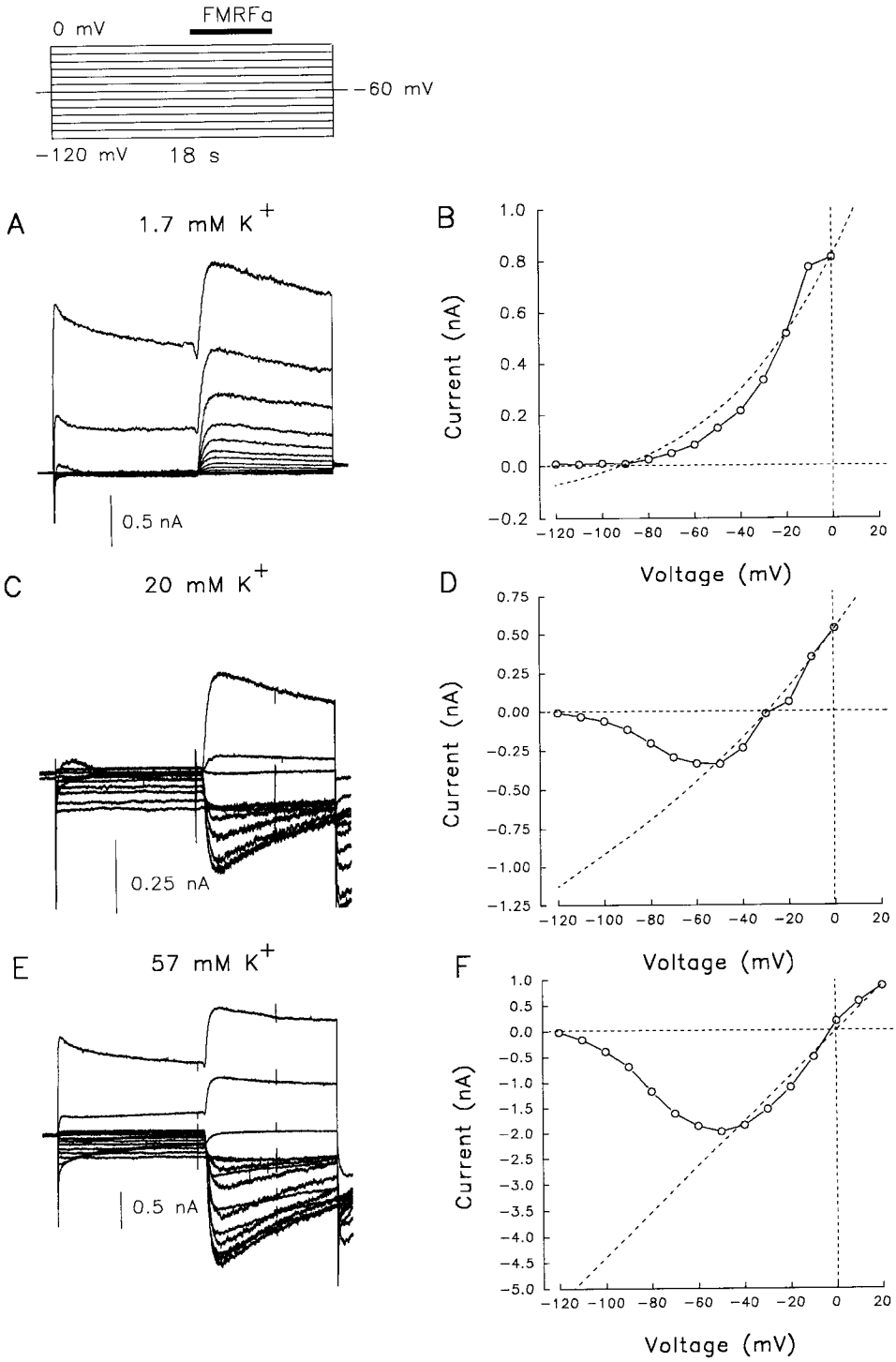

FIGURE 2. $[K]_o$ dependence of the current–voltage relation of the FMRFa response. Pulse protocol: thin lines indicate voltage steps (ranging from −120 to 0 mV in 10-mV increments; in *E* also, steps to +10 and +20 mV were applied) from the holding potential of −60 mV, bar indicates timing of the FMRFa pulse. Subsequent pulses were separated by 60-s intervals at −60 mV. (*A*) FMRFa responses measured in 1.7 mM $[K]_o$. Initial parts of the current traces show that at −20, −10, and 0 mV the test pulse elicits a voltage-dependent response. FMRFa is applied 10 s after the onset of the test pulse when the voltage-dependent response has reached a steady state. (*B*) Current voltage plot of the FMRFa responses in 1.7 mM $[K]_o$. FMRFa response amplitudes were measured as the difference between the maximal current amplitude during FMRFa application and the current level just before FMRFa was applied. The dotted line is the Goldman-Hodgkin-Katz equation (see Hille, 1994) fitted to the data, indicating the nonlinearity of the I-V curve expected to result from rectification due to asymmetric $[K^+]_o$ conditions. *C* and *D* are like *A* and *B*, but with $[K]_o$ = 20 mM. The theoretical reversal potential for K^+ is −29 mV. *E* and *F* are like *A* and *B*, but with $[K]_o$ = 57 mM; the theoretical reversal potential is −3 mV. All plots show representative examples.

potentials below −60 mV (in spite of the increasing driving force) and the lack of responses at potentials below −120 mV in both salines imply that the K^+ channels involved in this response are, to a certain extent, voltage dependent.

To assess the steepness of the voltage dependence, activation curves were constructed from the I-V data, plotting the conductance against the applied voltage. The conductance was calculated from the maximum current amplitude and the driving force for potassium. The driving force was calculated using the theoretical reversal potential (−92 mV) for the experiments in standard HBS (1.7 mM K^+) and the experimentally determined K^+ reversal potentials for 20 and 57 K^+-HBS.

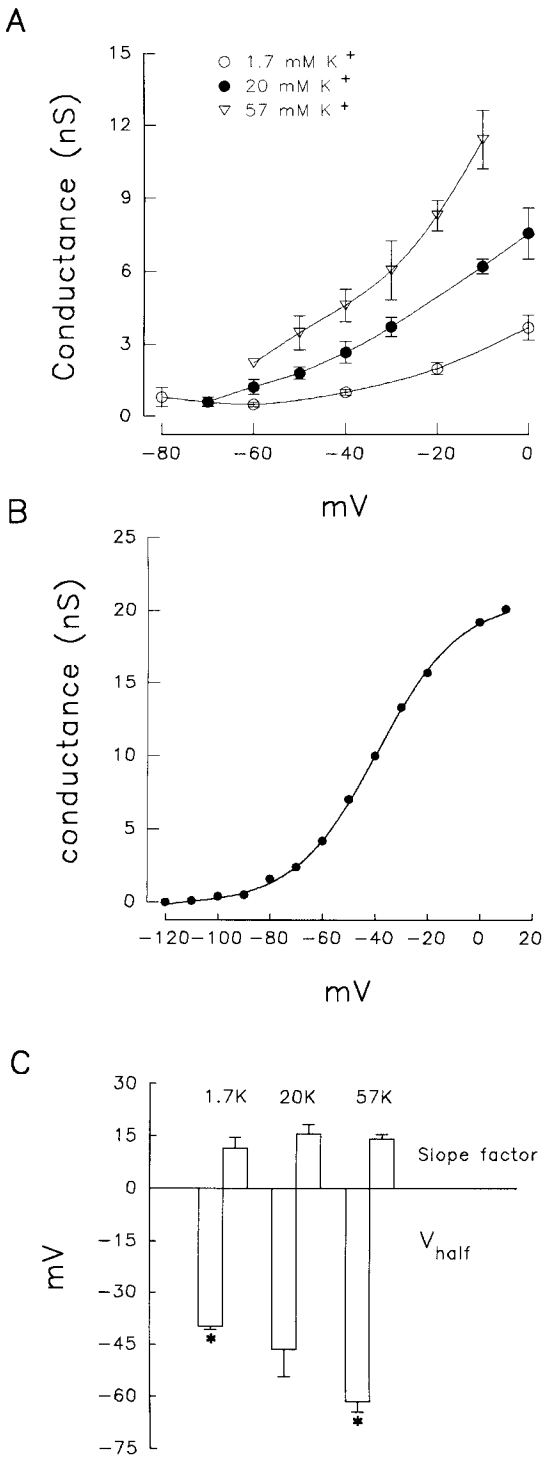

FIGURE 3. Voltage dependence of activation of the FMRFa-induced K^+ current. (*A*) Conductance (calculated as current amplitude divided by driving force; see text) is plotted against voltage for three different $[K^+]_o$ (as indicated). All plots are averages of three experiments, in each of which all three $[K^+]_o$ were tested on a single cell. (*B*) Example of an activation curve from a single cell obtained as described in *A*, but now for a wider voltage range (−120 to +10 mV) and with 10-mV increments between successive steps. $[K^+]_o$ = 20 mM. Fitted to the data is a Boltzmann curve: $G = G_{max}/[1+ \exp^{((Vhalf - Vm)/Sf)}]$ with G = Conductance, G_{max} = maximal conductance, V_m = membrane potential, V_{half} = membrane potential of half maximal conductance, Sf = slope factor, indicating the voltage sensitivity as the voltage necessary for an e-fold change in conductance. In this experiment, 50% activation occurred at V_{half} = 39 mV and the slope factor Sf = 15.6 mV. (*C*) $[K^+]_o$ dependence of V_{half} and the slope factor Sf determined in experiments as shown in *B*. V_{half} increases with $[K^+]_o$ while Sf remains constant (n = 4 for $[K^+]_o$ = 1.7 and $[K^+]_o$ = 57, n = 3 for $[K^+]_o$ = 20). *Significant difference.

To be able to measure the I-V relations for all three K^+ concentrations in one cell, a reduced protocol (−80 to 0 mV), shortening the duration of the experiment, was used. In three experiments, such a reduced I-V protocol was applied and the results of these three experiments were pooled. Plots of the mean conductance against voltage (Fig. 3 *A*) show that the conductance depends on (*a*) the membrane potential and (*b*) the extracellular K^+ concentration. In low potassium (1.7 mM K^+), where only outward currents occur, the conductance is lowest. With high extracellular K^+ concentrations, yielding mainly inward currents, the conductance is largest.

For further analysis, more complete I-V data (−120 to 0 mV) from different cells (two K^+ concentrations per cell) were compared. In most experiments it was not possible to isolate $I_{K\text{-}F}$ at potentials >0 mV since at these potentials large voltage-gated current responses occur that are to some extent also affected by FMRFa (Brussaard et al., 1990, 1991; Dreijer et al., 1995). To compare the conductances in the different K^+ concentrations, the data were fitted with a single Boltzmann equation (Fig. 3 *B*). These experiments confirm the above results, that the conductance is both voltage and $[K^+]_o$ dependent. The potential of maximal activation, V_{half}, differed significantly between 1.7 and 57 mM K^+, being highest in 1.7 (−39.8 ± 0.9 mV) and lowest in 57 (−61.6 ± 3.0 mV) mM K^+ (Fig. 3 *C*; unpaired *t* test, $P < 0.01$; $n = 4$). The average slope factors (the voltage required for an e-fold change in conductance) were ~14 mV and did not differ significantly for 1.7, 20, or 57 mM K^+, indicating that the voltage sensitivity is not dependent on $[K]_o$. It should be noted, however, that while Fig. 2 clearly shows that the voltage dependence is much stronger than expected on the basis of asymmetric K^+ conditions, rectification may contribute to the voltage dependence observed in 1.7 and 20 mM K^+ salines (see also DISCUSSION).

To confirm the presumed voltage dependence of channel gating, we next determined the instantaneous current–voltage relationship of the FMRFa response using a tail current protocol. FMRFa responses were evoked at a fixed potential of −30 or −50 mV followed by a variable tail step ranging from 0 to −140 mV. The FMRFa-induced currents were obtained by subtracting

control responses from those in the presence of FMRFa (Fig. 4, *A* and *B*). The instantaneous I-V relation of $I_{K\text{-}F}$ was determined by measuring the current amplitude immediately after stepping to the tail potential. For comparison, the I-V relation was measured 80 ms after the start of the tail potential. In these experiments, saline with 20 mM $[K^+]_o$ was used. The instantaneous I-V relations did not show the decrease in current response at potentials <-60 mV, but considerable outward rectification remained (Fig. 4 *C*). The traces of the tail currents at potentials <-60 mV, however, revealed a rapid deactivation phase (Fig. 4 *B*). In accordance, the I-V relations at $t = 80$ ms regained the voltage dependence of the response at hyperpolarized membrane potentials (Fig. 4 *C*). Thus, channels that are opened by FMRFa at the test potential rapidly deactivate upon stepping to hyperpolarized tail potentials. This result demonstrates that voltage dependence stems from a step in channel gating. In addition, the instantaneous I-V relation shows that the current flow through the channels is outwardly rectifying. The outward rectification was stronger than predicted by the Goldman-Hodgkin-Katz equation on the basis of asymmetric ion concentrations (Fig. 4 *C*). Qualitatively similar results were obtained regardless of the potential at which the FMRFa response was first evoked (-10, -30, -40, -50, or -60 mV; $n = 7$ cells).

Activation kinetics of the channel. The kinetics of the response were slow. At 10^{-6} M, the current reached a maximum in almost a second and decayed within tens of seconds. At lower doses, the rise phase of the response was considerably prolonged (Fig. 1 *A*). The rise time of the response comprises ligand–receptor interaction, possibly cytoplasmic or membrane-bound signal transduction steps, and activation of the channel.

When FMRFa was applied at a voltage of -40 mV, the

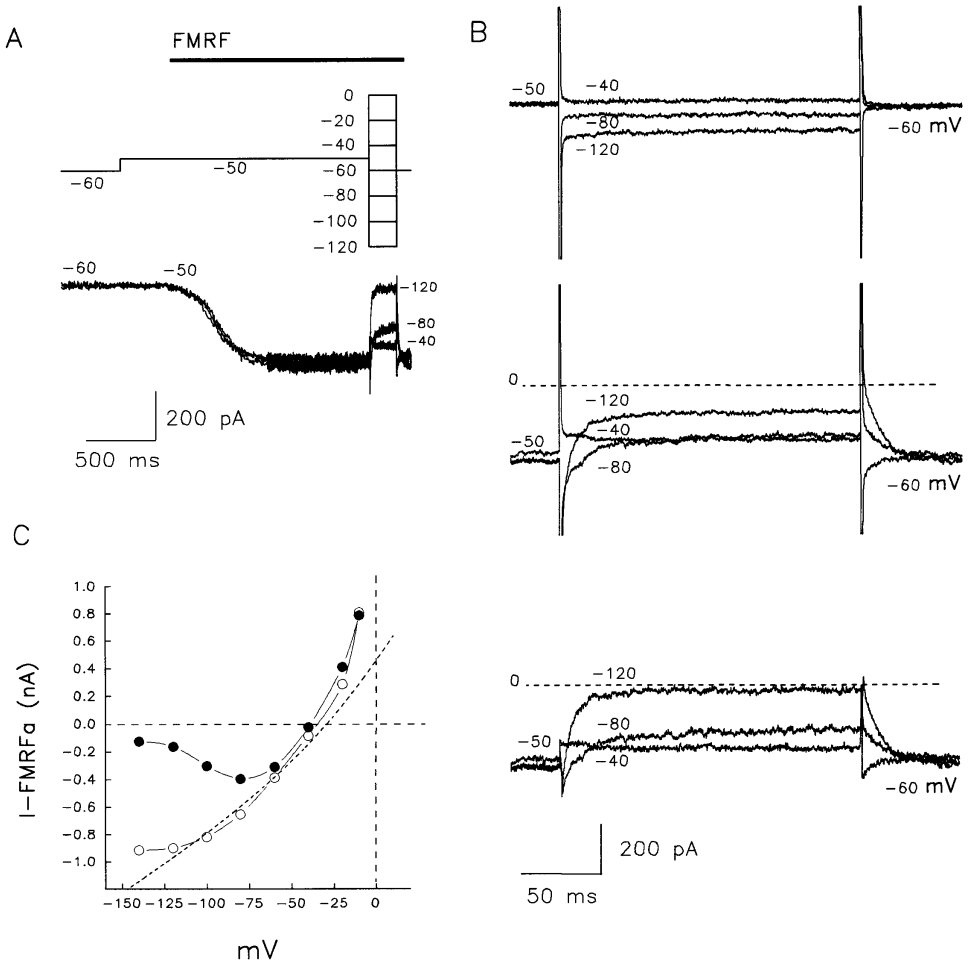

FIGURE 4. Tail currents and instantaneous current–voltage relation of $I_{K\text{-}F}$. (*A*) Pulse protocol: holding potential -60 mV; prepulse to -50 mV, during which $I_{K\text{-}F}$ was evoked, followed by a variable test pulse as indicated to record tail currents; finally, a step back to the holding potential. FMRFa was applied 1.8 s before onset of the tail potential until 0.5 s after ending the 200-ms tail potential. Intervals between successive responses lasted 2 min. Shown are the isolated responses upon stepping back to -120, -80, and -40 mV, obtained by subtraction of the recordings obtained without and with FMRFa application. (*B*) Same experiments as in *A*. Tail currents measured during the test pulse at potentials indicated. (*top*) Control recordings without FMRFa application. (*middle*) Tail-current responses recorded upon FMRFa application. (*bottom*) Isolated $I_{K\text{-}F}$ tail currents obtained by subtraction of control currents from the responses in the presence of FMRFa. At -120 mV, the tail current rapidly and almost completely deactivates; at -80 mV, partial deactivation occurs (note the steady state current level); and, at -40 mV, no deactivation occurs but the current immediately assumes its steady level. Note that upon stepping back to -60 mV the current amplitude increases again. The dotted line indicates zero current level. (*C*) Protocol as in *A* and *B*, but in this case $I_{K\text{-}F}$ was evoked during a prepulse to -30 mV. Plotted is the instantaneous current voltage relation of $I_{K\text{-}F}$ (○, measured as the maximum amplitude of the isolated tail currents). For comparison, the I-V relation measured at $t = 80$ ms is also shown (●), which reveals the normal voltage dependence. The dotted line is a fit by the Goldman-Hodgkin-Katz equation. Experiment performed in $[K^+]_o = 20$ mM. Sampling rate 5 kHz, filtering at 2 kHz.

response reached its maximum in 648 ± 42 ms (n = 15). Since the Y-tube system allowed application of FMRFa in ~170 ms (see MATERIALS AND METHODS), the application was not rate limiting. To investigate the activation kinetics of the channels, we employed the voltage dependence of the response, as illustrated in Fig. 5 *A*. FMRFa was applied at a voltage of −120 mV, a few seconds before a voltage step to −40 mV was made to activate the current. The rise time of $I_{K\text{-}F}$, evoked by the step to −40 mV, appeared to be much faster then.

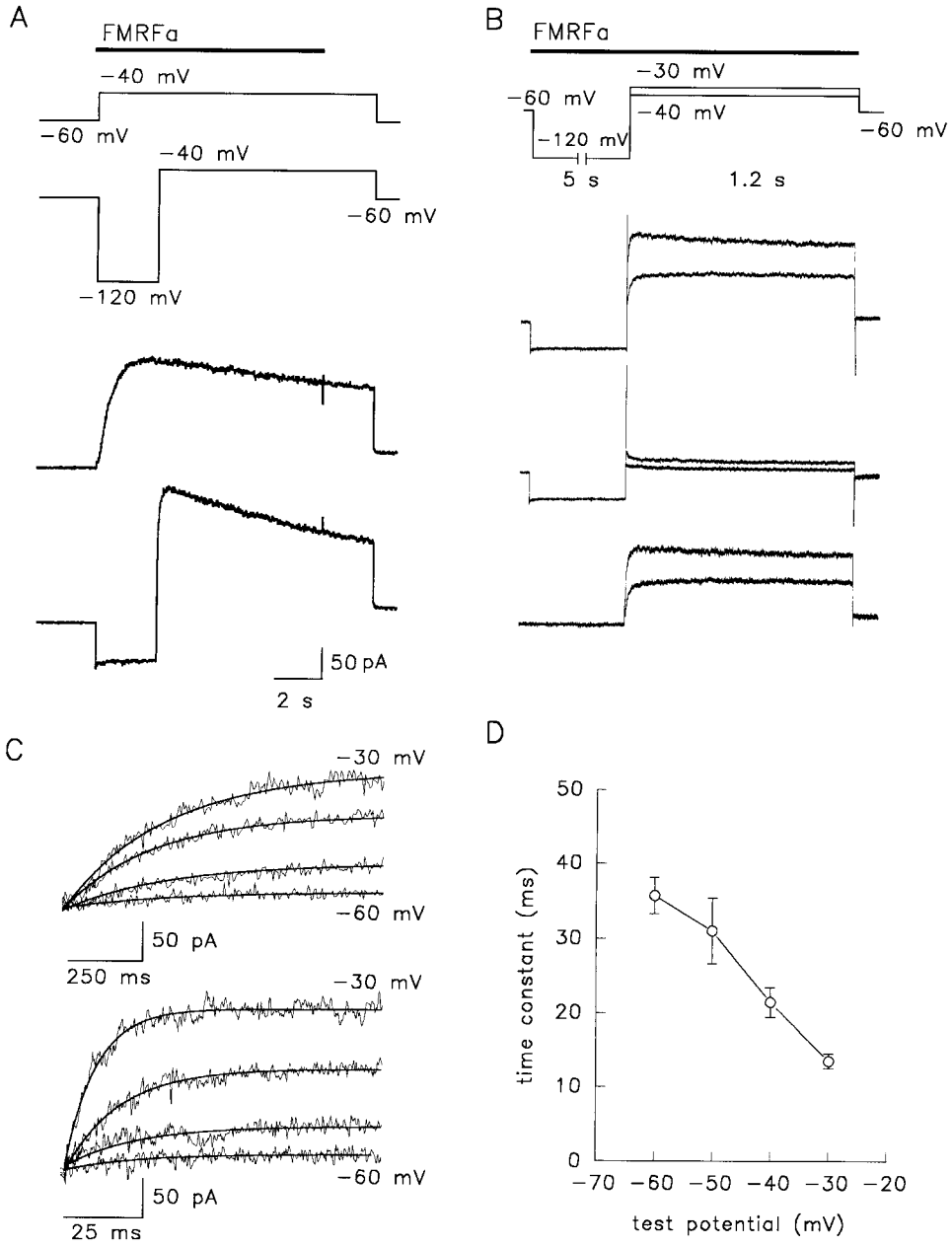

FIGURE 5. Activation kinetics of the FMRFa current response. (*A*) Pulse protocol: bar indicates FMRFa application, thin lines indicate voltage steps (*top:* from −60 to the test potential of −40 mV; *bottom:* from −60 to −120 (prepulse) followed by the step to −40 mV). Current traces are the corresponding responses. At −40 mV, FMRFa evokes a slowly activating outward current. When applied at −120 mV, FMRFa does not evoke a response, but the current is only activated when the voltage is subsequently stepped to −40 mV. However, the rate of activation in the latter case is much faster than upon application of FMRFa at −40 mV (rise times of 141 ± 16 and 648 ± 42 ms, respectively; n = 15; the former value being limited by the low sampling and filtering rate in these experiments). (*B*) Pulse protocol: bar indicates FMRFa application, thin lines indicate voltage steps (holding potential −60 mV, FMRFa application at −120 mV, and subsequent test pulses to test potentials of −40 and −30 mV. Duration of prepulse and test pulse as indicated. Test pulse responses were sampled at 5 kHz and filtered at 2 kHz. (*top*) Current responses obtained with application of FMRFa. (*middle*) Control current responses (without FMRFa). Note that control responses consist of a capacitive transient and the ohmic response due to the step from −120 to −40 or −30 mV, but that a time dependent, voltage gated component is not present or negligible. (*bottom*) Isolated $I_{K\text{-}F}$ responses, obtained by subtracting the control traces from the responses in the presence of FMRFa. (*C*) Onset kinetics of $I_{K\text{-}F}$ without and with a prepulse to −120 mV. (*top*) Protocol like in *B* but without a prepulse to −120 mV and test pulses lasting 6.2 s to potentials ranging from −60 to −30 mV in 10-mV steps. FMRFa application timed at the onset of the test pulse. Sampling and filtering as in *B*. Shown are isolated $I_{K\text{-}F}$ responses during the first second of the test pulse, obtained by subtraction (see *B*). Superimposed are monoexponential fits, all having a time constant of ~300 ms. (*bottom*) Protocol as in *B* (including prepulse to −120 mV), but with test pulses to potentials ranging from −60 to −30 mV in 10-mV steps. Family of isolated current responses to FMRFa during the first 100 ms of the test pulse obtained by subtraction. Superimposed are single exponential fits to the rising phases of the responses. Time constants in this experiment were 38.3 ms at −60 mV, 37.7 ms at −50 mV, 19.5 ms at −40 mV, and 10.1 ms at −30 mV. (*D*) Time constants of activation of $I_{K\text{-}F}$ are voltage dependent. Plotted are the average time constants of activation of $I_{K\text{-}F}$ as a function of voltage. Data obtained from experiments as illustrated in the lower plots of *C*. n = 7 except for −60 mV where n = 4, because in three cases responses were too small for reliable fitting.

These results suggest that the rise time upon direct application of FMRFa at −40 mV is determined by relatively slow processes as receptor activation and subsequent signal transduction steps. If FMRFa is applied at −120 mV, the receptor will be activated and signal transduction starts. Channel opening, however, will only occur upon the subsequent voltage step to a depolarized voltage.

In a separate series of experiments, a similar approach was used to assess activation kinetics quantitatively (Fig. 5, *B–D*). The signal-to-noise ratio obtained with the high sampling rate and cut off filtering frequency used limited the analysis to potentials of ≥−60 mV. To avoid contamination with voltage-gated currents that may be influenced by FMRFa, we did not use data of −20 mV and more positive potentials (see also Fig. 5 *B*, which illustrates that the voltage-gated currents activated by steps to −40 or −30 mV are sufficiently small to be ignored). Thus, the analysis was restricted to the voltage range from −60 up to −30 mV. The time constants of activation were determined by fitting single exponentials to the isolated $I_{K\text{-}F}$ current traces obtained by subtraction of responses in the absence and presence of FMRFa using a prepulse protocol as described above (Fig. 5, *B* and *C*). For comparison, Fig. 5 *C* also shows $I_{K\text{-}F}$ current traces that were obtained by applying FMRFa with the cell at the test potential. Whereas the latter traces revealed activation time constants of ~300 ms at each potential, the fast responses to test pulses after FMRFa application at −120 mV had activation time constants that were >10 times faster and decreased at more depolarized test potentials. The results are summarized in Fig. 5 *D*. The time constants at −50 (31.0 ± 13.21 ms), −40 (21.4 ± 6.1 ms), and −30 (13.5 ± 3.1 ms) mV were significantly different (paired *t* test, $P < 0.02$, $n = 7$). We conclude from these data that channel opening is fast and voltage dependent.

Inactivation of $I_{K\text{-}F}$

When FMRFa is continuously applied, the current reaches its maximum and then slowly decreases (Figs. 1 and 5). The processes underlying this decrease might be receptor desensitization, desensitization at another level in the signal-transduction route, or channel inactivation. To discriminate between these processes, we examined whether the decay rate depends on concentration or voltage. If desensitization of the receptor is involved, the decay will depend on the concentration of the ligand. If the underlying process concerns channel inactivation, the time constant of the decay should not depend on concentration but possibly on voltage.

Concentration independence of current decay. The decay of $I_{K\text{-}F}$ during 30- or 45-s applications of 10^{-6} and 5×10^{-8} M FMRFa was measured at −30 and −40 mV (Fig. 6 *A*). The time course of the decay was fitted with a single exponential curve. The mean values of the time constants thus obtained were all ~14 s and did not significantly differ for the two concentrations at either potential (two way analysis of variance, ANOVA, $P > 0.05$, $n = 4$ for each treatment; Fig. 6 *B*). Since, even in 45-s current traces, the current decay was incomplete and ~25% of the peak amplitude remained, we also determined the percentage decline at $t = 30$ s after the onset of the response for the two concentrations. These percentages (mean values of ~67%) also did not differ significantly (two way ANOVA, $P >> 0.05$, data not shown). These data show that, at least in this range, neither the decay rate nor the amount of decay is dependent on concentration. This suggests that the current decay is not caused by desensitization of the receptor or a following signal transduction step.

Voltage dependence of inactivation. There was no significant difference in the decay rates of $I_{K\text{-}F}$ responses evoked with 10^{-6} M FMRFa at −30 (13.0 ± 2.2 s, $n = 4$), −40 (14.2 ± 3.2 s, $n = 4$), or −50 (14.7 ± 2.8 s, $n = 3$)

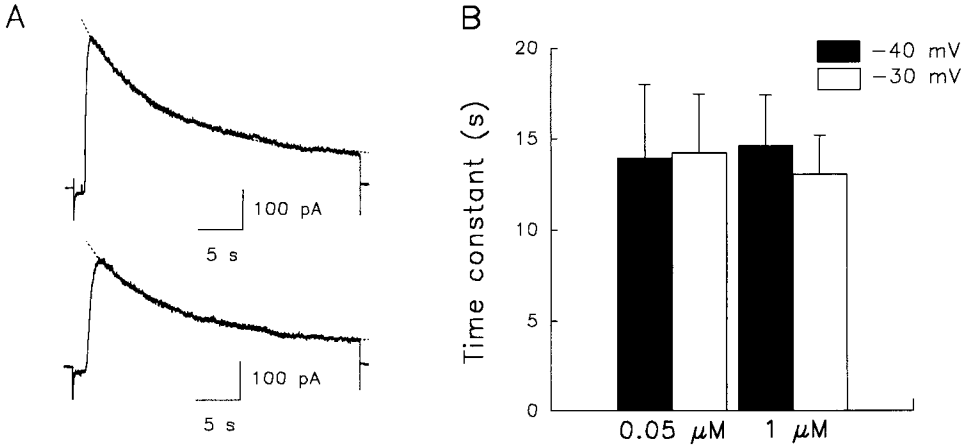

FIGURE 6. Lack of effect of FMRFa concentration on decay rates. (*A*) Current responses to 10^{-6} M (*top*) and 5×10^{-8} M (*bottom*) FMRFa at −30 mV. Single exponentials were fitted to the decay phase of the traces. The time constant was 9.4 s for 10^{-6} M and 9.9 s for 5×10^{-8} M. Data from the same cell. (*B*) Average decay time constants (±SD) of current responses to 10^{-6} and 5×10^{-8} M FMRFa at −30 and at −40 mV ($n = 4$ for both concentrations and both potentials).

mV (ANOVA, $P > 0.05$). To measure the voltage dependence of inactivation over the complete voltage range of −120 to −30 mV, a prepulse protocol was used. In this protocol, prepulses of 15-s duration to various potentials (ranging from −120 to 0 mV in 10-mV steps) were given, followed by an 8-s step to the test potential of −40 mV. FMRFa was applied 1 s after the start of the prepulse. The decrease in current amplitude at −40 mV as a function of increasing prepulse potential was used as a measure for the amount of inactivation that has taken place during the prepulse (Fig. 7). To allow complete recovery from inactivation, each test pulse was followed by an interval of 80 s, during which the cell was kept at −80 mV holding potential. The largest current response at −40 mV was obtained with a prepulse to −120 mV. Increasing the voltage of the prepulse resulted in smaller currents at the test pulse of −40 mV, with on average the lowest current at −50 mV. Further increase of the prepulse voltage did not induce stronger inactivation. This is in line with the above result that the decays at −50, −40, and −30 mV did not differ (see also Fig. 6 *B*). Fig. 7 *B* summarizes the dependence of inactivation on prepulse voltage ($n = 7$).

To confirm the absence of inactivation at hyperpolarized potentials, FMRFa was applied for 20 min at −120 mV, a voltage at which the FMRFa channel is not activated. During this time, short (1.5 s) voltage steps to −40 mV were made every 60 s. These voltage steps activated $I_{K\text{-}F}$ but were too short to cause significant inactivation. Over the time course of 20 min of FMRFa application, no decrease in amplitude of successive current responses was observed ($n = 4$; not shown).

To measure the time course of inactivation at hyperpolarized voltages, prepulses of varying duration were applied and followed by a test pulse to −40 mV. Prepulses to −120, −100, and −80 mV were given and FMRFa was applied from 1 s after the start of the prepulse until the end of the test pulse (Fig. 8 *A*). The amplitude of $I_{K\text{-}F}$ during the test pulse was measured and plotted against the duration of the FMRFa application preceding the test pulse (Fig. 8 *B*). At −120 mV, the current hardly inactivated. At higher voltages, inactivation progressively increased. The increase in the rate and degree of inactivation at potentials increasing from −120 to −80 mV was consistently observed in four cells, thus confirming the voltage dependence of the inactivation rate.

The above results all point to voltage-dependent inactivation of $I_{K\text{-}F}$.

Recovery from inactivation. With the application method we used, FMRFa was washed away in 4 s. The cells, however, had to recover for ~60 s from an application of 2–5 s. With smaller intervals, the response to a subsequent application of FMRFa was decreased. Apparently, recovery from inactivation is very slow at the holding potential of −60 mV that was used in most experiments.

Recovery did not take place when, during FMRFa application, a voltage step to −120 mV was made in order to shut the channel. This was tested in a protocol where, under continuous application of FMRFa, the

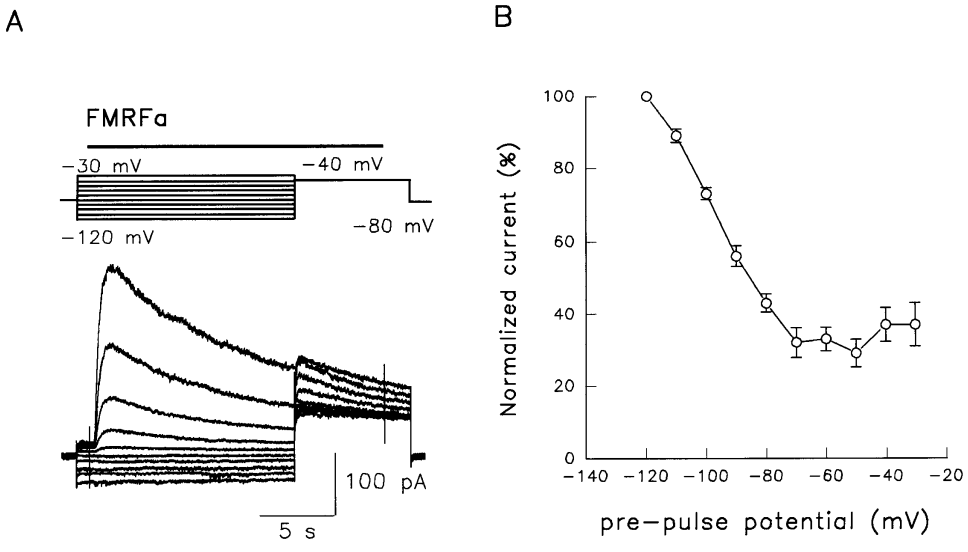

FIGURE 7. Voltage dependence of inactivation. (*A*) Pulse protocol: bar indicates FMRFa pulse, thin lines indicate voltage steps. From a holding of −80 mV, a 15-s prepulse to potentials ranging from −120 to −30 mV preceded the test pulse to −40 mV. Subsequent pulse pairs were separated by 80-s intervals. Thus, prepulse inactivation in the presence of FMRFa was tested. Current traces show the corresponding responses. Since the experiment was performed in 1.7 mM $[K]_o$, only prepulses to ≥−70 mV elicited an FMRFa response. The test pulse to −40 mV activated the largest current when preceded by a prepulse to −120 mV. Increasing the prepulse voltage decreased the response at −40 mV, showing that inactivation is stronger at more depolarized potentials. (*B*) Normalized current amplitude during the test pulse plotted against prepulse potential (data normalized with respect to the amplitude obtained with a prepulse to −120 mV; $n = 7$; means ± SEM values are given).

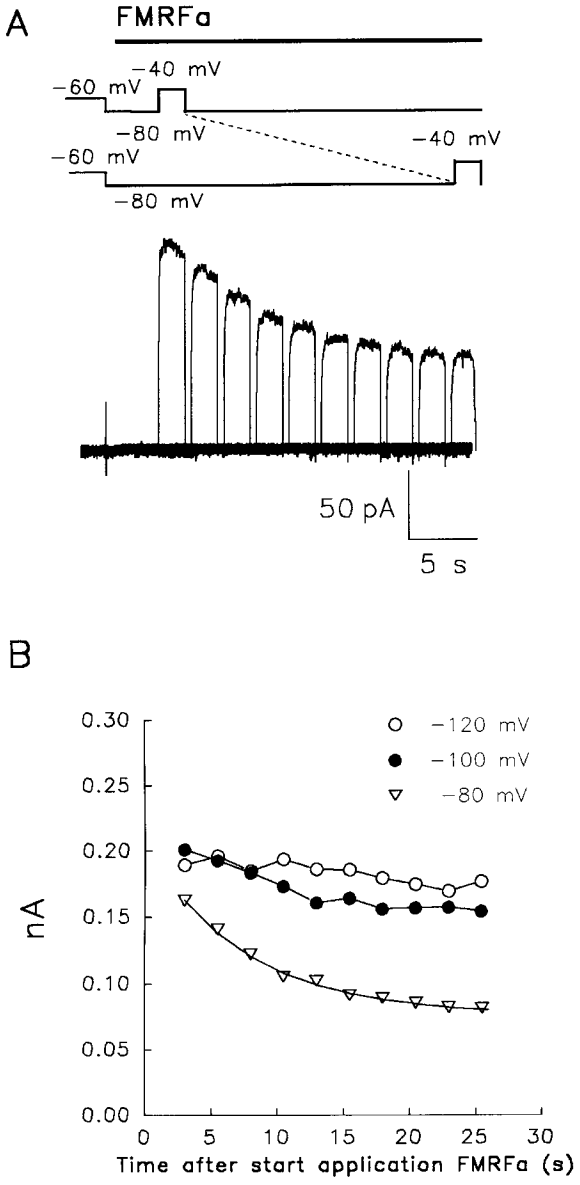

FIGURE 8. Time course of inactivation. (*A*) Pulse protocol: bar indicates FMRFa application, thin lines indicate voltage. A prepulse of variable length (increasing from 4 to 26.5 s in 2.5-s steps) to −80 mV was followed by a test pulse to −40 mV. FMRFa was applied 1 s after the start of the prepulse to yield FMRFa pulses of 3 to 25.5 s. Subsequent FMRFa pulses were separated by 60-s periods. Thus, the time dependence of inactivation of the response at −80 mV in the presence of FMRFa was measured. Superimposed current traces show the decrease in response amplitude when the duration of the interval at −80 mV is increased. (*B*) Plot of the current amplitudes against duration of interval of FMRFa application at a given potential preceding the start of the test pulse. Plots are given for −80 (data from *A*), −100, and −120 mV. Inactivation at −120 and −100 mV was too slow to be fitted reliably. At −80 mV, inactivation was well described by a time constant of 7.5 s, indicating that in this cell inactivation was relatively rapid. All data from the same cell.

clamp potential was first set at −40 mV to induce inactivation of the response, then at −120 mV for up to 10 min, and finally again at −40 mV. The final step back to −40 mV did not reveal recovery of the response (n = 3; not shown). It follows that recovery from inactivation only took place when FMRFa was washed away.

Pharmacological Properties of $I_{K\text{-}F}$

Basic pharmacological properties of $I_{K\text{-}F}$ were assessed by eliciting responses in the absence and presence of the blocker of choice in the external medium, using the protocol illustrated in Fig. 1. In this way, 4-AP, tetraethylammonium (TEA), Ba^{2+}, Cd^{2+}, and Cs^{+} were tested. The decrease in response amplitude was measured after 10 min of incubation with the blocker. Furthermore, we tested the effect of intracellular application of TEA by including the blocker in the pipette medium. In these experiments, block was measured as the decline in response amplitude over the first 30 min after establishing the whole cell configuration. Table I lists the results. In short, (nearly) complete block of $I_{K\text{-}F}$ is obtained with 10 mM internal TEA, 10 mM extracellular TEA, 1 mM 4-AP, and 1 mM Ba^{2+}. Approximately 50% block was obtained with 0.5 mM external Cd^{2+} and 1 mM external Cs^{+}. Apart from the block by 4-AP, all blocking effects were rapidly (within 10 min) reversed upon wash.

Signal Transduction

Second messenger involvement. The slow onset kinetics of the FMRFa response may be explained by signal transduction steps preceding channel activation. To illustrate the involvement of second messengers, we employed the voltage dependence of the response. FMRFa was applied for 2 s at −120 mV and, following a variable time interval after washing away FMRFa, the channel was activated by stepping to −40 mV (Fig. 9 *A*). The $I_{K\text{-}F}$ responses progressively decreased with increasing time intervals. Fig. 9 *B* shows that the relation between

TABLE I

Pharmacological Properties of $I_{K\text{-}F}$

Blocker	Percent block	Reversible	n	V_m	$[K]_O$
10 mM TEA in	100	Not tested	4	−30 mV	1.7 mM
10 mM TEA ext	78±11	+	3	−30 mV	1.7 mM
1 mM 4-AP ext	96±2	− or ±	5	−20, −30 mV	1.7 mM
1 mM Cs^{+} ext	44±6	+	5	−60 mV	57 mM
1 mM Ba^{2+} ext	100	+	3	−30 mV	1.7 mM
0.5 mM Cd^{2+} ext	47±11	+	4	−20 mV	1.7 mM

Percent block was measured after a 10-min incubation except for TEA in, in which case block was measured after a 30-min recording; data are derived from responses at indicated potentials. Note that Cs^{+} block was studied in high K^{+} saline. All blocking effects were reversible within 10 min of wash, except block by 4-AP, which did not reverse or only partially reversed within this period. in, intracellular application; ext, bath application.

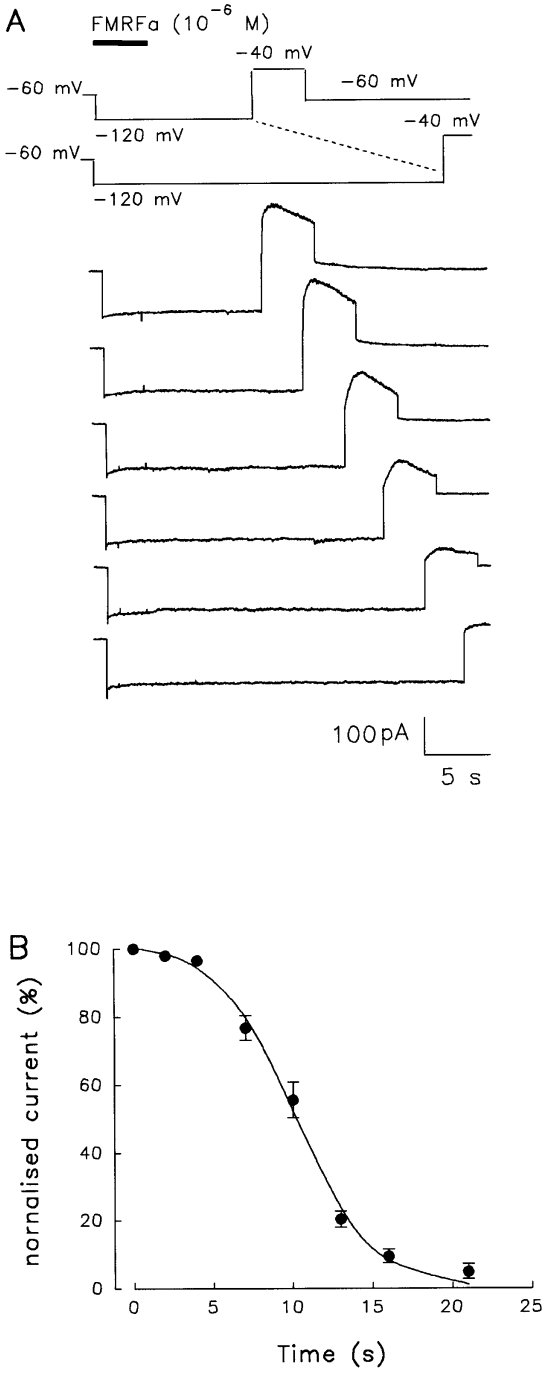

FIGURE 9. Second messenger involvement in FMRFa responses. (*A*) Protocol: bar indicates FMRFa pulse, thin lines indicate voltage steps. FMRFa was applied for 2 s at a potential of −120 mV. After an interval of variable duration in the absence of FMRFa, a test pulse to −40 mV was applied. Holding potential −60 mV. Successive current responses show that the FMRFa responses decrease when the interval between application and test pulse is increased, but a response can be evoked up to 20 s after application of the peptide. (*B*) Plot of the normalized current amplitude against duration of the interval between ending FMRFa application and start of the test pulse to −40 mV. Data points are the averages of seven experiments.

response amplitude and time interval duration follows a sigmoid curve ($n = 7$ cells). Most likely, this curve reflects the time-dependent decrease in availability of the relevant second messenger. Current activation remained possible, however, up to 20 s after FMRFa had been washed away.

G-protein coupling. To study whether the FMRFa response involves activation of G-proteins, we asked whether GTPγS interfered with the response. GTPγS, a nonhydrolyzable GTP analogue, is expected to cause persistent activation of the α subunit and prevent its binding to the βγ subunit. For this experiment, FMRFa was applied for 2 s at a test potential of −40 mV, and this application was repeated every 60 s. During the 60-s interval, the cell was kept at a holding potential of −60 mV. Without GTPγS, but with GTP in the pipette, this procedure can be continued for 20–30 min without losing current (Fig. 10 *A*; $n = 5$). With GTPγS instead of GTP in the pipette, we saw a gradual rise in holding current, arising because the responses did not completely reverse upon washing away FMRFa. This increase in holding current reached a maximum and then reversed slowly. The most obvious effect of GTPγS, however, was a steady decline in amplitude of the responses to FMRFa (Fig. 10 *B*; $n = 7$). The effect of GTPγS took 10–15 min to establish, a time course that reasonably meets the expectation for a cell of 50-μm diameter and a series resistance of ∼6 MΩ (Pusch and Neher, 1988). When the same cell was sealed again with a pipette containing GTP instead of GTPγS, the effect of GTPγS appeared to reverse slowly (Fig. 10 *B*). The observation that intracellular dialysis with GTPγS, replacing endogenous GTP, led to incomplete wash out of the current responses and a gradual rise in holding current, is explained by continuous activation of the signal transduction pathway by the GTPγS-bound G-protein. The reversal of this phenomenon and the time-dependent decrease of the FMRFa-activated current is explained by assuming that continuous activation of the signal transduction pathway will induce channel inactivation. Similar results were obtained with presumed G-protein-coupled responses to dopamine in *Lymnaea* neurones (Van Tol-Steye et al., 1997).

Coupling to arachidonic acid metabolism. Three blockers that interfere with enzymes involved in the formation or degradation of arachidonic acid (AA) were used to find out whether AA or its metabolites are involved in the coupling of the FMRFa receptor to the channel. These experiments were performed by 2-s applications of FMRFa at a test potential of −40 mV repeated every 60 s, before and after application of the relevant blocker. First step in the arachidonic acid metabolism is the release of AA from membrane phospholipids, a reaction that is catalyzed by the enzyme phospholipase A_2 (Axelrod et al., 1988). This enzyme can be effectively

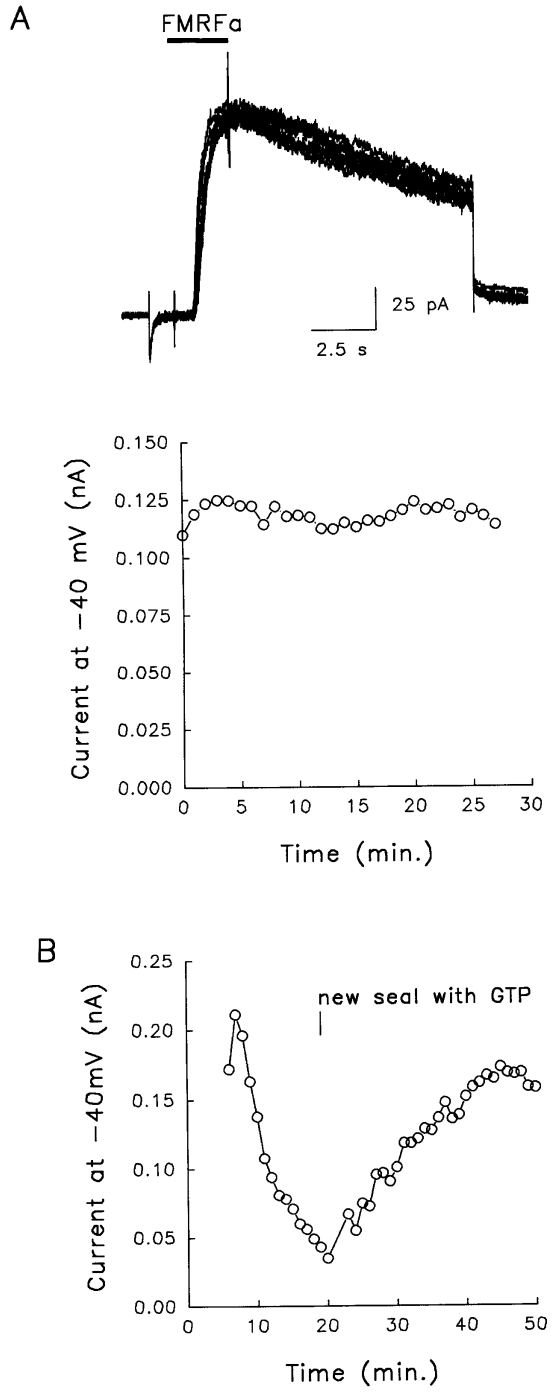

FIGURE 10. G-protein dependence of the FMRFa response. Protocol: FMRFa was applied for 2 s, 1 s after a step to −40 mV. Holding potential −60 mV; interval between FMRFa pulses, 60 s. (*A*) Control experiment, illustrating that, using this protocol, the FMRFa response remains constant for over 25 min. (*top*) Current traces; (*bottom*) plot of current amplitude against time. Each data point is the response to a single FMRFa pulse. (*B*) Effect of GTPγS on the responses to FMRFa. Plot of current amplitude against time. Initially, the pipette saline contained GTPγS, but after 20 min this pipette was withdrawn and the cell was whole cell voltage clamped with a new pipette containing standard internal saline with GTP. A slow recovery (~80% in 25 min) of the response is observed. Data in *A* and *B* are from different cells.

blocked by 4-bromophenacyl-bromide (Piomelli et al., 1987). Applying 4-bpb (10^{-5} M) by bath perfusion leads to irreversible rundown of the current (Fig. 11 *A*; $n = 5$), suggesting that arachidonic acid is involved in this response.

After formation of arachidonic acid, it is metabolized via three different routes. The first enzymes in these routes are either 12-lipoxygenase, 5-lipoxygenase (yielding eicosanoids), or cyclo-oxygenase (yielding prostaglandins). To determine which of these routes is involved in the FMRFa response, we tested the actions of nordihydroguairetic acid, which blocks lipoxygenases, and indomethacin, which blocks cyclo-oxygenase without affecting lipoxygenase activity (Piomelli et al., 1987). Bath perfusion with NDGA caused a gradual rundown of the response (Fig. 11 *B*; $n = 3$). However, indomethacin did not have an effect on the FMRFa response (Fig. 11 *C*; $n = 3$). These experiments suggest that a lipoxygenase, rather than cyclo-oxygenase, is involved in the intracellular signaling process.

To test whether arachidonic acid is indeed the messenger through which FMRFa activates the channel, we examined whether exogenously applied AA interferes with the FMRFa response. Application of arachidonic acid (5×10^{-4} M) to the cell at a test potential of −40 mV activated an outward current that was as large as or even larger than the current activated by FMRFa at that voltage ($n = 5$). Fig. 12 *A* shows examples of the AA-induced current. In this experiment, arachidonic acid was applied for 50 s at −40 mV and this application was repeated at intervals of 120 s. Each subsequent application resulted in a larger current than the one before. Apparently, the AA-induced current response does not completely reverse within 120 s, possibly due to incomplete wash out.

To test whether the same channels that are opened by FMRFa are also opened by AA, we examined whether the currents to AA and to FMRFa show summation. Arachidonic acid was applied for 120 s at −60 mV. FMRFa was then applied in 5-s pulses during voltage steps to −40 mV at the end of the AA pulse and at increasing intervals after the AA pulse. AA induced an outward current of ~100 pA at the holding potential of −60 mV, and of ~350 pA upon stepping to −40 mV. The first $I_{K\text{-}F}$ response, directly after the 120-s AA pulse, was smallest, while subsequent $I_{K\text{-}F}$ responses progressively increased with time after AA application (Fig. 12 *B*). This result indicates that AA and FMRFa address the same channels.

DISCUSSION

The present results define a voltage-dependent, neuronal K^+ current that requires the presence of the neuropeptide FMRFa to be activated. Its biophysical properties exclude, however, that $I_{K\text{-}F}$ arises through facilita-

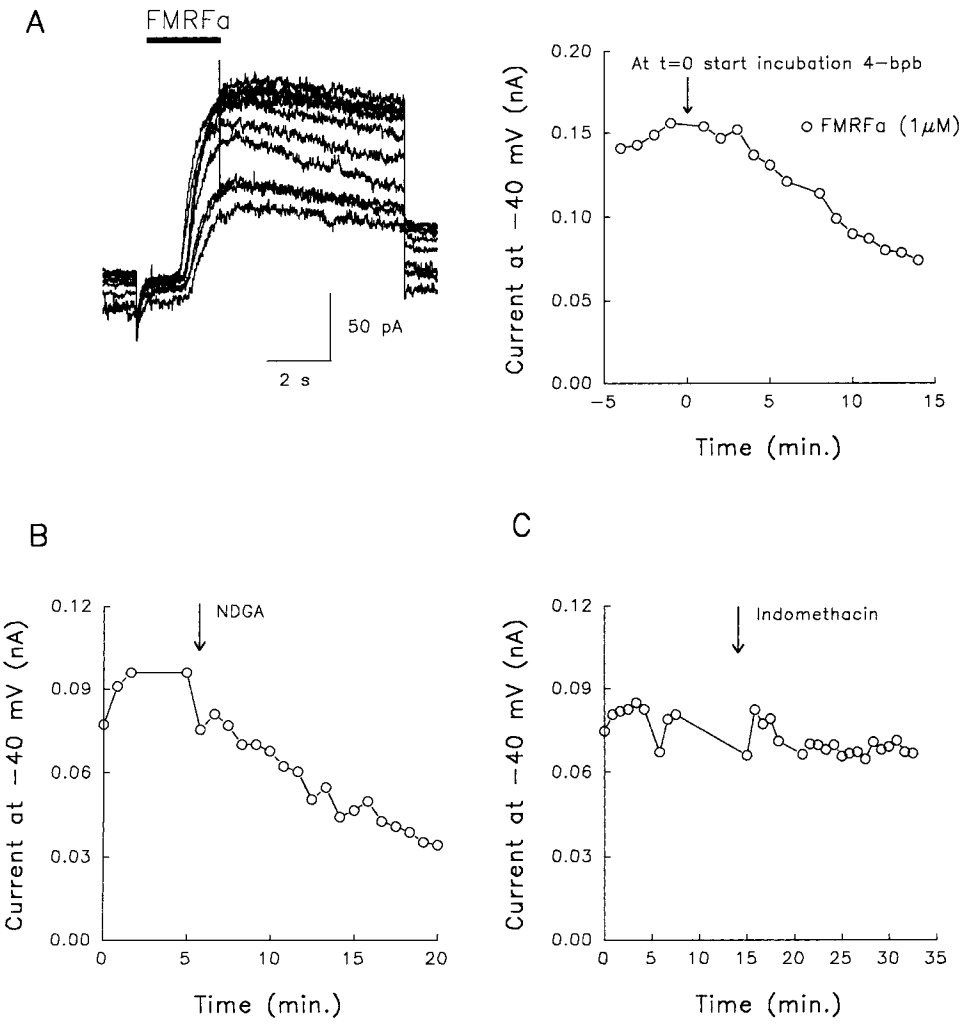

FIGURE 11. Involvement of PLA_2 and lipoxygenase in signal transduction of the FMRFa response. Protocol as in Fig. 10. (*A*, *left*) Four control pulses of FMRFa were given in standard HBS, followed by a series of pulses in HBS with 10^{-5} M 4-bpb. During this series, the response amplitude steadily declined. (*right*) Time course of the blocking effect of 4-bpb on the FMRFa response. (*B*) Blocking effect of NDGA on the FMRFa response. (*C*) Lack of effect of indomethacin on the FMRFa response. (*A–C*) Representative examples, different cells.

tion of classical voltage-gated currents by FMRFa. These voltage-gated currents have a much faster activation and inactivation rate (A-current) and/or their voltage dependence is strongly different, with V_{half} being at least 40 mV more positive (delayed rectifier and Ca^{2+}-dependent K^+ current), and the slope of the activation curves being steeper (Kits and Lodder, unpublished data). Activation of $I_{K\text{-}F}$ will result in a hyperpolarization and a decrease in excitability of the cell. Thus, the current is functionally similar to other receptor-driven K^+ currents, such as vertebrate neuronal K^+ currents activated by dopamine, opiates, and a number of other transmitters acting on G-protein-coupled receptors, and the FMRFa-activated S-K current in *Aplysia* and other molluscs (see references in INTRODUCTION). In addition, if spiking is not completely suppressed by FMRFa, $I_{K\text{-}F}$ will quicken spike repolarization. However, unlike what has been reported for S-K channels (Critz et al., 1991; Hochner and Kandel, 1992), we have no indications that $I_{K\text{-}F}$ is active in the absence of FMRFa and it is therefore unlikely to play a role in spike repolarization under control conditions. In spite of the functional similarities, $I_{K\text{-}F}$ clearly differs from these channel types in biophysical and pharmacological characteristics (see below), indicating that it represents a novel K^+ current (sub)type.

Signal Transduction of the FMRFa Response

The present results strongly suggest that the K^+ channels involved in the FMRFa response are activated through the arachidonic acid pathway. Inhibition of PLA_2 by 4-bpb, as well as inhibition of lipoxygenase by indomethacin, strongly reduced the response to FMRFa, suggesting that block of these enzymes interrupts the signal transduction. On the other hand, NDGA, which blocks cyclo-oxygenase, did not affect the response, suggesting that lipoxygenase products (eicosanoids) are instrumental in the response to FMRFa. This signal transduction pathway is similar to the way in which S-K channels are activated (Belardetti and Siegelbaum, 1988; Buttner et al., 1989). Our experiments did not address the question whether additional signal trans-

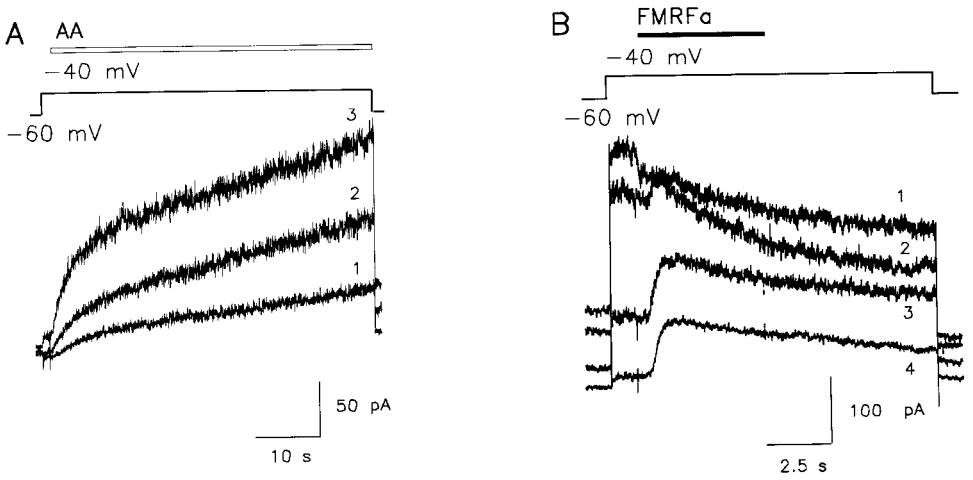

FIGURE 12. Involvement of arachidonic acid in signal transduction of the FMRFa response. (*A*) Superimposed responses to arachidonic acid. AA was applied during three successive 50-s pulses to −40 mV (*open bar*, AA application; *thin line*, voltage step; holding potential during the 2-min intervals was −60 mV). AA induced an outward current that continued to grow during the 50-s application. Also, successive responses to AA increased in amplitude and rate of rise (traces *1–3*). (*B*) In this experiment, a cell was loaded with AA for 120 s. Upon ending AA application, the cell was stepped to −40 mV. Note that this step increases the outward current in a similar way as occurs when FMRFa application is followed by step to −40 mV. FMRFa (*black bar*), applied 1 s later, failed to evoke a response (trace *1*). An FMRFa pulse 1 s after stepping to −40 mV was then repeated at different moments in time during the decay of the AA-induced current. Traces *2–4* show that when the AA current decreases, the response to FMRFa increases again. (*A* and *B*) Different cells.

duction pathways converge upon this channel. Previously, it was shown, however, that the FMRFa response was not affected by increasing cAMP (Brussaard et al., 1988). Still, like S-K channels, the $I_{K\text{-}F}$ channels may be subject to cAMP regulation, but FMRFa may antagonize and override possible cAMP effects.

Kinetics of the FMRFa Response

Activation of a second messenger-mediated signal transduction route provides an explanation for the slow onset of the response (∼650 ms) when FMRFa is applied at a voltage of −40 mV. The rate of rise of the response is much faster when channel activation at −40 mV is preceded by application of FMRFa at −120 mV, at which potential only receptor activation and second messenger formation will take place. The subsequent step to −40 mV elicits the current response with a much shorter rising phase (<<100 ms). These observations suggest that activation of the arachidonic acid signal transduction pathway accounts for the major part (several hundreds of milliseconds) of the activation time of the response, while the final step of channel opening proceeds fast. In addition, channel opening is a voltage-dependent step with activation time constants decreasing at more depolarized test potentials.

Inactivation

The amount and the rate of decay of the $I_{K\text{-}F}$ response do not depend on the FMRFa concentration applied, but they are clearly dependent on voltage (see Figs. 7 and 8). This makes it very likely that the decay is caused by voltage-dependent inactivation of the channels and not by a desensitization process acting on a preceding signal transduction step or the FMRFa receptor. This conclusion is supported by previous observations that the suppression of the excitability by FMRFa of CDCs in situ (Brussaard et al., 1988) and the inhibition of the voltage-gated Na^+ and Ca^{2+} currents (Brussaard et al., 1990, 1991; Dreijer et al., 1995) do not desensitize during prolonged incubation with FMRFa (>10 min). The underlying assumption that a single FMRFa receptor is involved in all responses is supported by their similar concentration dependence ($ED_{50} \cong 2 \times 10^{-8}$ M for $I_{K\text{-}F}$) and by the identical agonist structure requirements of the different responses to FMRFa (Brussaard et al., 1989). Thus, the voltage dependence of $I_{K\text{-}F}$ decay and the lack of desensitization of the other responses to FMRFa all suggest that the reduction of $I_{K\text{-}F}$ during prolonged or repeated application of FMRFa is not due to desensitization but to voltage-dependent inactivation.

Voltage Dependence

The current–voltage and the conductance–voltage relationships derived from them show a moderate but clear voltage dependence of the FMRFa-operated current. Boltzmann plots yielded a slope factor of 12–16, indicating that the voltage dependence arises from 1.5–2 equivalent gating charges in the channel. Our analysis of the voltage dependence of conductance will, to some extent, overestimate the voltage dependence of channel gating in 1.7 and 20 mM K^+ because the contribution of Goldman-Hodgkin-Katz rectification is neglected. (This objection does not hold for the 57 K^+ condition, yielding nearly symmetrical K^+ concentrations, where Goldman-Hodgkin-Katz rectification is negligible.) Comparison of the experimentally obtained

data of Fig. 3 with the predictions obtained by calculating conductance on the basis of Goldman-Hodgkin-Katz I-V curves in 20 and 1.7 K^+ salines, pointed out that the contribution of rectification to the overall voltage dependence in the voltage range of −80 to 0 mV is ~25% in 20 K^+, but >50% in 1.7 K^+. Nevertheless, even in 1.7 $[K]_o$, rectification fails to explain the voltage dependence completely.

Our conclusion that channel gating is voltage dependent is based on the following evidence: (*a*) a clear voltage dependence of conductance was observed in nearly symmetrical K^+ conditions. (*b*) The instantaneous I-V relation (reflecting conductance properties of the opened channels) failed to show the voltage dependence of the response, but revealed only outward rectification. In addition, clear voltage-dependent deactivation was observed during tail currents at <−60 mV. (*c*) While activation is normally slow, fast activation was observed upon stepping to −40 mV after applying FMRFa to a cell at −120 mV. This suggests that only channel opening is impeded at −120 mV. (*d*) Activation time constants decreased from ~36 to ~13 ms over the voltage range of −60 to −30 mV. (*e*) A voltage-dependent step in receptor activation is ruled out since a step to −40 mV after a transient application of FMRFa with the cell at −120 mV (thus failing to generate a current response) still evokes a response, even if the step to −40 mV is given up to 20 s after washing out FMRFa.

Interestingly, we found that the voltage dependence shifts to more negative potentials with increasing external K^+ concentrations. In addition, the conductance voltage plots reveal that the FMRFa-activated conductance increases with increasing $[K^+]_o$. These phenomena are probably related to outward rectification due to asymmetric K^+ concentrations that will limit current amplitudes (and thus conductance derived from this) at voltages near the reversal potential. The outward rectification is most clear from the instantaneous current–voltage relation (Fig. 4). Goldman-Hodgkin-Katz fits do not completely describe this relationship, suggesting that, in addition to asymmetrical K^+ concentrations, intrinsic channel properties may contribute to it. Furthermore, it is possible that at 1.7 and 20 mM $[K^+]_o$, the external potassium concentration limits the absolute value of the conductance for inward current, thus contributing to the observed decreased conductance at decreased $[K^+]_o$.

The above findings imply three possible mechanisms that reduce the amplitude of the FMRFa-induced current at low potentials: (*a*) voltage dependence of activation, (*b*) outward rectification due to asymmetrical K^+ concentrations and, possibly, intrinsic channel properties, and (*c*) submaximal conductance of inward currents at low $[K^+]_o$. These mechanisms explain the lack of inward currents at potentials of <−80 mV in 1.7 mM $[K]_o$. At the same time, however, these mechanisms will reinforce FMRFa-induced inhibition in depolarized or active cells.

Relation of $I_{K\text{-}F}$ to Other Receptor-driven Channels

Clearly, $I_{K\text{-}F}$ does not classify as a GIRK or classical inward rectifier. Firstly, our results imply that PLA_2 activity is required for the FMRFa response to occur, which excludes direct gating of the channels by a G-protein subunit. Although, for instance, cardiac K_{ACh} channels are stimulated by lipoxygenase products, this pathway is not used by muscarinic stimulation and most likely this pathway stimulates K_{ACh} channels by acting on the G-protein involved (Kurachi et al., 1989, 1992). Secondly, the voltage-dependence curves of $I_{K\text{-}F}$ do not reveal inward rectification. Thirdly, the voltage dependence of $I_{K\text{-}F}$ channel gating, like that of inward rectifiers, depends on $[K]_o$, but in the opposite way. While inward rectifiers shift their voltage dependence towards more positive potentials with increasing $[K^+]_o$, due to relief of internal Mg^{2+} block by an inward K^+ current (see Hille, 1994), increasing $[K^+]_o$ shifts the voltage dependence of $I_{K\text{-}F}$ towards more negative potentials and increases the conductance. In fact, as discussed above, outward rectification of $I_{K\text{-}F}$ will contribute to this phenomenon. The appearance of inward currents may depend on competition between K^+ and a blocking ion in the outer mouth of the channel, only resulting in inward current flow when $[K^+]_o$ is sufficiently high. The steepness of voltage dependence falls between that of classical IRKs (or inward rectifier K^+ channels) (2.5–5) and that of GIRKs like the muscarinic K^+ channel (0.5–1).

Functionally, as well as regarding the signal transduction pathway coupling the channels to the FMRFa receptor, $I_{K\text{-}F}$ closely resembles the S-K current. However, both biophysical and pharmacological differences between $I_{K\text{-}F}$ and $I_{S\text{-}K}$ are observed. The voltage dependence of activation and inactivation constitutes a major difference in biophysical properties. Regarding the voltage dependence of activation, $I_{K\text{-}F}$ is characterized by a more hyperpolarized voltage range (at low $[K^+]_o$ $V_{1/2} = -40$ mV for $I_{K\text{-}F}$ vs. >0 mV for $I_{S\text{-}K}$) and a steeper slope (14 mV for $I_{K\text{-}F}$ vs. 30–100 mV for $I_{S\text{-}K}$) (Shuster et al., 1991). Pollock et al. (1985) measured the I-V relation of $I_{S\text{-}K}$ also in high K^+ saline, and observed outward rectification but no U-shaped I-V curve. Similarly, the S-K-like channel studied by Brezina et al. (1987) only displays Goldman-Hodgkin-Katz rectification. Whereas these results point to differences with $I_{K\text{-}F}$, it should be noted that many studies on $I_{S\text{-}K}$ concern single channel recordings (Shuster et al., 1991), rather than macroscopic currents (but see Klein et al., 1982; Pollock et al., 1985; Baxter and Byrne, 1989). The fast channel activation kinetics of $I_{K\text{-}F}$ constitute another biophysical difference from $I_{S\text{-}K}$, the latter being characterized by

slow activation, even at depolarized potentials (−20 mV) (Klein et al., 1982; Baxter and Byrne, 1989). Finally, our data strongly suggest voltage-dependent inactivation of $I_{K\text{-}F}$, which does not hold for the S-K current (Klein et al., 1982; Pollock et al., 1985; Baxter and Byrne, 1989).

Pharmacologically, $I_{K\text{-}F}$ differs from $I_{S\text{-}K}$ in many respects. Externally applied 4-AP (1 mM), TEA (10 mM), and Ba (1 mM) all completely blocked $I_{K\text{-}F}$, whereas these agents do not affect $I_{S\text{-}K}$ in concentrations up to 10 mM (Pollock et al., 1985; Shuster and Siegelbaum, 1987; Baxter and Byrne, 1989). Also, internal TEA is a more effective blocker of $I_{K\text{-}F}$ (~75% block of $I_{K\text{-}F}$ at 10 mM vs. a K_d of 40 mM for $I_{S\text{-}K}$). Furthermore, $I_{K\text{-}F}$ is blocked for ~50% by 0.5 mM Cd^{2+}, which contrasts the lack of block of $I_{S\text{-}K}$ by the related divalent ion Co^{2+}, even at 10 mM (Shuster and Siegelbaum, 1987). The higher sensitivity of $I_{K\text{-}F}$ to internal and external TEA may to some extent be caused by the circumstance that the ionic strength of *Lymnaea* salines is much less than that of *Aplysia* salines (total ion concentration ~120 vs. ~1,200 mM, respectively). However, the discrepancies with respect to the effects of 4-AP and external divalent ions point to real differences in channel properties. The strong block by divalent ions Ba^{2+} and Cd^{2+} is reminiscent of divalent ion block in classical voltage-gated K^+ channels, where gating requires interaction with Ca^{2+} ions (Armstrong and Lopez Barneo, 1987; Armstrong and Miller, 1990; Begenisich, 1988). Thus it is likely that the divalent ion block of $I_{K\text{-}F}$ relates to its voltage dependence and marks a difference with $I_{S\text{-}K}$.

In spite of these differences, at the molecular level channels carrying $I_{K\text{-}F}$ may be closely related to S-K channels. Interestingly, a possible molecular candidate for the S-K channel (aKv5.1) is not related to the inward rectifiers but to the *Shaker* family (Zhao et al., 1994).

Divergence of FMRFa Responses

FMRFa has a strong inhibitory effect on the CDCs. It rapidly suppresses discharges of CDCs, both in situ and in isolated CDCs (Brussaard et al., 1988). The inhibition by FMRFa in CDCs involves at least three different actions: inhibition of the voltage-activated sodium current (Brussaard et al., 1990, 1991*a*), suppression of the slowly inactivating HVA calcium current (Dreijer et al., 1995), and activation of a potassium current (Brussaard et al., 1988; and this paper). The simultaneous activation of three cooperative inhibitory mechanisms explains the strong inhibition of the CDCs by FMRFa.

Although multiple receptors for FMRFa and related −RFamides are assumed to exist in the molluscan nervous system (Cottrel and Davies, 1987; Payza, 1987), it was concluded from structure activity studies that the multiple responses to FMRFa in CDCs are mediated by a single receptor type (Brussaard et al., 1989). This implies that the divergence of the FMRFa responses may occur at the level of the G-protein or the primary effector of the G-protein. A common signal transduction route is unlikely since the suppression of calcium channels is not mediated by the arachidonic acid pathway and probably involves a direct effect of the G-protein on the channel (Dreijer et al., 1995), while stimulation of K^+ channels takes place via the arachidonic acid route. No data are available on the route by which sodium channels are affected. Divergence of FMRFa effects was also observed in bag cell neurons of *Aplysia californica*, where FMRFa inhibits discharges by activation of both potassium and chloride currents and suppression of a voltage-dependent calcium current (Fisher et al., 1993) and in *Helisoma* B5 neurons, where presynaptic inhibition by FMRFa is brought about by modulation of calcium channels and of the secretory machinery (Man-Son-Hing et al., 1989) and activation of a K^+ current (Bahls et al., 1992). In these cells it is not known whether a single or multiple receptors are involved.

The strong inhibitory action of FMRFa on CDCs is spread over the CDC network by three different mechanisms. First, FMRFamidergic axons come in close apposition to the CDCs at several spots, suggesting numerous synaptic or synapselike contacts with the CDCs (Brussaard et al., 1988). Secondly, the CDC network is electrotonically coupled, allowing effective spread of especially slow phenomena like the FMRFa-induced hyperpolarization (Vlieger et al., 1980). The results of the present work imply a third route. Arachidonic acid, used as second messenger in the signal transduction route, may diffuse from its site of formation to adjacent cells, thus spreading the inhibition.

We thank Dr. A.B. Brussaard, Dr. H.D. Mansvelder, Dr. P. van Soest, and Prof. T.A. de Vlieger for comments on the manuscript.
M.J. Veerman was on a grant of the Netherlands Organization for Scientific Research.

Original version received 15 April 1997 and accepted version received 28 August 1997.

References

Armstrong, C.M., and J. Lopez Barneo. 1987. External calcium ions are required for potassium channel gating in squid neurons. *Science (Wash. DC).* 236:712–714.

Armstrong, C.M., and C. Miller. 1990. Do voltage-dependent K^+ channels require Ca^{2+}? A critical test employing a heterologous expression system. *Proc. Natl. Acad. Sci. USA.* 87:7579–7582.

Axelrod, J., R.M. Burch, and C.L. Jelsema. 1988. Receptor-mediated activation of phospholipase A_2 via GTP-binding proteins: arachidonic acid and its metabolites as second messengers. *Trends Neurosci.* 11:117–123.

Bahls, F.H., J.E. Richmond, W.L. Smith, and P.G. Haydon. 1992. A lipoxygenase pathway of arachidonic acid metabolism mediates FMRFamide activation of a potassium current in an identified neuron of *Helisoma. Neurosci. Lett.* 138:165–168.

Baxter, D.A., and J.H. Byrne. 1989. Serotonergic modulation of two potassium curents in the pleural sensory neurons of *Aplysia. J. Neurophysiol.* 62:665–679.

Begenisich, T. 1988. The role of divalent cations in potassium channels. *Trends Neurosci.* 11:270–273.

Belardetti, F., and S.A. Siegelbaum. 1988. Up- and down-modulation of single K^+ channels by distinct second messengers. *Trends Neurosci.* 11:232–238.

Belkin, K.J., and T.W. Abrams. 1993. FMRFamide produces biphasic modulation of the LFS motor neurons in the neural circuit of the siphon withdrawal reflex of *Aplysia* by activating Na^+ and K^+ currents. *J. Neurosci.* 13:5139–5152.

Bolshakov, V.U., S.A. Gapon, A.N. Katchman, and L.G. Magazanik. 1993. Activation of a common potassium channel in molluscan neurones by glutamate, dopamine and muscarinic agonist. *J. Physiol. (Camb.).* 468:11–33.

Brezina, V., C.G. Evans, and K.R. Weiss. 1994. Activation of K current in the accessory radula closer muscle of *Aplysia californica* by neuromodulators that depress its contractions. *J. Neurosci.* 14: 4412–4432.

Brezina, V., R. Eckert, and C. Erxleben. 1987. Modulation of potassium conductances by an endogenous neuropeptide in neurones of *Aplysia californica. J. Physiol. (Camb.).* 382:267–290.

Brown, A.M. 1990. G-proteins and potassium currents in neurons. *Annu. Rev. Physiol.* 52:215–242.

Brown, A.M., and L. Birnbaumer. 1990. Ionic channels and their regulation by G-protein subunits. *Annu. Rev. Physiol.* 52:197–213.

Brussaard, A.B., A. Ter Maat, T.A. de Vlieger, and K.S. Kits. 1990. Inhibitory modulation of neuronal voltage-dependent sodium current by Phe-Met-Arg-Phe-amide. *Neurosci. Lett.* 111:325–332.

Brussaard, A.B., J.C. Lodder, A. Ter Maat, T.A. de Vlieger, and K.S. Kits. 1991. Inhibitory modulation by FMRFamide of the voltage gated sodium current in identified neurones in *Lymnaea stagnalis. J. Physiol. (Camb.).* 441:385–404.

Brussaard, A.B., K.S. Kits, A. Ter Maat, J. van Minnen, and P.J. Moed. 1988. Dual inhibitory action of FMRFamide on peptidergic neurons controlling egg laying behavior in the pond snail. *Brain Res.* 447:35–51.

Brussaard, A.B., K.S. Kits, and A. Ter Maat. 1989. One receptor type mediates two independent effects of FMRFa on neurosecretory cells of *Lymnaea. Peptides (Tarryt.).* 10:289–297.

Buttner, N., S.A. Siegelbaum, and A. Volterra. 1989. Direct modulation of Aplysia S-K^+ channels by 12-lipoxygenase metabolite of arachidonic acid. *Nature (Lond.).* 342:553–555.

Clapham, D.E. 1994. Direct G-protein activation of ion channels? *Annu. Rev. Neurosci.* 17:441–464.

Cottrell, G.A., and N.W. Davies. 1987. Multiple receptor sites for a molluscan peptide (FMRFamide) and related peptides of *Helix. J. Physiol. (Camb.).* 382:51–68.

Critz, S.D., D.A. Baxter, and J.H. Byrne. 1991. Modulatory effects of serotonin, FMRFamide, and myomodulin on the duration of action potentials, excitability, and membrane currents in tail sensory neurons of *Aplysia. J. Neurophysiol.* 66:1912–1926.

de Vlieger, T.A., K.S. Kits, A. Ter Maat, and J.C. Lodder. 1980. Morphology and electrophysiology of the ovulation hormone producing neuroendocrine cells of the freshwater snail *Lymnaea stagnalis. J. Exp. Biol.* 84:259–271.

Dreijer, A.M.C., S. Verheule, and K.S. Kits. 1995. Inhibition of a slowly inactivating high-voltage-activated calcium current by the neuropeptide FMRFa in molluscan neuroendocrine cells. *Invert. Neurosci.* 1:75–86.

Einhorn, L.C., and G.S. Oxford. 1993. Guanine nucleotide binding proteins mediate D_2 dopamine receptor activation of a potassium channel in rat lactotrophs. *J. Physiol. (Lond.).* 462:563–578.

Einhorn, L.C., K.A. Gregorson, and G.S. Oxford. 1991. D_2 dopamine receptor activation of potassium channels in identified rat lactotrophs: whole cell and single channel recordings. *J. Neurosci.* 11:3727–3737.

Endo, S., S.D. Critz, J.H. Byrne, and S. Shenolikar. 1995. Protein phosphatase-1 regulates outward K^+ currents in sensory neurons of *Aplysia calcifornica. J. Neurochem.* 64:1833–1840.

Fisher, T., C.-H. Lin, and L.K. Kaczmarek. 1993. The peptide FMRFamide terminates a discharge in *Aplysia* bag cell neurons by modulating calcium, potassium and chloride conductances. *J. Neurophys.* 69:2164–2173.

Greiff, G.J., Y.-J. Lin, and J.E. Freedman. 1995*a*. Role of cyclic AMP in dopamine modulation of potassium channels on rat striatal neurons: regulation of a subconductance state. *Synapse (NY).* 21: 275–277.

Greiff, G.J., Y.-J. Lin, J.-C. Liu, and J.E. Freedman. 1995*b*. Dopamine-modulated potassium channels on rat striatal neurons: specific activation and cellular expression. *J. Neurosci.* 15:4533–4544.

Hille, B. 1994. Ionic channels of excitable membranes. 2nd ed. Sinauer Associates, Sunderland, MA. pp. 341–484.

Hochner, B., and E.R. Kandel. 1992. Modulation of a transient K^+ current in the pleural sensory neurons of *Aplysia* by serotonin and cAMP: implications for spike broadening. *Proc. Natl. Acad. Sci. USA.* 89:11476–11480.

Kehoe, J.S. 1995. Glutamate activates a K^+ conductance increase in *Aplysia* neurons that appears to be independent of G proteins. *Neuron.* 13:691–702.

Kim, K.-M., Y. Nakajima, and S. Nakajima. 1995. G protein coupled inward rectifier modulated by dopamine agonists in cultured substantia nigra neurons. *Neuroscience.* 69:1145–1158.

Klein, M., J. Camardo, and E.R. Kandel. 1982. Serotonin modulates a specific potassium current in the sensory neurons that show presynaptic facilitation in *Aplysia. Proc. Nat. Acad. Sci. USA.* 79: 5713–5717.

Kunkel, M.T., and E.G. Peralta. 1995. Identification of domains conferring G-protein regulation on inward rectifier potassium channels. *Cell.* 83:443–449.

Kurachi, Y. 1995. G protein regulation of cardiac muscarinic potassium channel. *Am. J. Physiol.* 269:821–830.

Kurachi, Y., H. Ito, T. Sugimoto, T. Shimizu, I. Miki, and M. Ui. 1989. Arachidonic acid metabolites as intracellular modulators of the G protein-gated cardiac K^+ channel. *Nature (Lond.).* 337: 555–557.

Kurachi, Y., R.T. Tung, H. Ito, and T. Nakajima. 1992. G protein activation of cardiac muscarinic K^+ channels. *Prog. Neurobiol. (Oxf.).* 39:229–246.

Logothetis, D.E., Y. Kurachi, J. Galper, E.J. Neer, and D.E. Clapham. 1987. The $\beta\gamma$ subunits of GTP-binding proteins acti-

vate the muscarinic K^+ channel in heart. *Nature (Lond.)*. 325:321–326.

Man-Son-Hing, H., M.J. Zoran, K. Lukowiak, and P.G. Haydon. 1989. A neuromodulator of synaptic transmission acts on the secretory apparatus as well as on ion channels. *Nature (Lond.)*. 341:237–239.

Nichols, C.G., and W.J. Lederer. 1991. Adenosine triphosphate-sensitive potassium channels in the cardiovascular system. *Am. J. Physiol.* 261:H1675–H1686.

Payza, K. 1987. FMRFamide receptors in *Helix aspersa*. *Peptides (Tarryt.)*. 8:1065–1074.

Piomelli, D., A. Volterra, N. Dale, S.A. Siegelbaum, E.R. Kandel, J.H. Schwartz, and F. Berlardetti. 1987. Lipoxygenase metabolites of arachidonic acid as second messengers for presynaptic inhibition of *Aplysia* sensory cells. *Nature (Lond.)*. 328:38–43.

Pollock, J.D., L. Bernier, and J.S. Camardo. 1985. Serotonin and cyclic adenosine 3′:5′-monophosphate modulate the S potassium current in sensory neurons in the pleural ganglion of *Aplysia*. *J. Neurosci.* 5:1862–1871.

Pusch, M., and E. Neher. 1988. Rates of diffusional exchange between small cells and a measuring patch pipette. *Pflügers Arch.* 411:204–211.

Raffa, R.B. 1988. The action of FMRFamide (Phe-Met-Arg-Phe-NH_2) and related peptides on mammals. *Peptides (Tarryt.)*. 9:915–922.

Sasaki, K., and M. Sato. 1987. A single GTP-binding protein regulates K^+-channels coupled with dopamine, histamine and actylcholine receptors. *Nature (Lond.)*. 325:259–262.

Shuster, M.J., and S.A. Siegelbaum. 1987. Pharmacological characterization of the serotonin-sensitive potassium channel of *Aplysia* sensory neurons. *J. Gen. Physiol.* 90:587–608.

Shuster, M.J., J.S. Camardo, and S.A. Siegelbaum. 1991. Comparison of the serotonin-sensitive and Ca^{2+}-activated K^+ channels in *Aplysia* sensory neurons. *J. Physiol. (Camb.)*. 440:601–621.

Sweatt, J.D., A. Volterra. B. Edmonds, K.A. Karl, S.A. Siegelbaum, and E.R. Kandel. 1989. FMRFamide reverses protein phosphorylation produced by 5-HT and cAMP in *Aplysia* sensory neurons. *Nature (Lond.)*. 342:275–278.

Takano, M., and A. Noma. 1993. The ATP-sensitive K^+ channel. *Prog. Neurobiol. (Oxf.)*. 41:21–30.

Terzic, A., A. Jahangir, and Y. Kurachi. 1995. Cardiac ATP-sensitive K^+ channels: regulation by intracellular nucleotides and K^+ channel-opening drugs. *Am. J. Physiol.* 38:C525–C545.

Terzic, A., R.T. Tung, A. Inanobe, T. Katada, and Y. Kurachi. 1994. G-proteins activate ATP-sensitive K^+ channels by antagonizing the ATP-dependent gating. *Neuron*. 12:885–893.

Vandorpe, D.H., D.L. Small, A.R. Dabrowski, and C.E. Morris. 1994. FMRFa and membrane stretch as activators of the *Aplysia* S-channel. *Biophys. J.* 66:46–58.

Van Tol-Steye, H., J.C. Lodder, R.J. Planta, H. van Heerikhuizen, and K.S. Kits. 1997. Convergence of multiple G-protein-coupled receptors onto a single type of potassium channel. *Brain Res.* In press.

Vreugdenhil, E., J.F. Jackson, T. Bouwmeester, A.B. Smit, J. van Minnen, H. van Heerikhuizen, J. Klootwijk, and J. Joosse. 1988. Isolation, characterization, and evolutionary aspects of a cDNA clone encoding multiple neuropeptides involved in the stereotyped egg-laying behavior of the freshwater snail, *Lymnaea stagnalis*. *J. Neurosci.* 8:4184–4191.

Wickman, K., and D.E. Clapham. 1995. Ion channel regulation by G-proteins. *Physiol. Rev.* 75:865–885.

Wickman, K.D., J.A. Iniguez-Lluhi, P.A. Davenport, R. Taussig, G.B. Krapivinsky, M.E. Linder, A.G. Gilman, and D.E. Clapham. 1994. Recombinant G-protein βγ-subunits activate the muscarinic gated atrial potassium channel. *Nature (Lond.)*. 368:255–257.

Zhao, B., F. Rassendren, B.-K. Kaang, Y. Furukawa, T. Kubo, and E.R. Kandel. 1994. A new class of non-inactivating K^+ channels from *Aplysia* capable of contributing to the resting potential and firing patterns of neurons. *Neuron*. 13:1205–1213.